

A11101-729039

NBSIR 80-1631

NAT'L INST. OF STAND & TECH R.I.C.



A11105 037109

**Reference**

NBS  
Publi-  
cations

# ANALYSIS OF LIQUID VOLUME AND LIQUID MASS FRACTIONS AT COEXISTENCE FOR PURE FLUIDS

---

Lambert John Van Poolen, Ph. D.†

Thermophysical Properties Division  
National Engineering Laboratory  
National Bureau of Standards  
Boulder, Colorado 80303

† Guest Worker: Professor of Engineering  
Calvin College  
Grand Rapids, Michigan 49506

QC

100

.U56

80-1631

1980

May 1980



NBSIR 80-1631

QC 50  
1056  
no. 80-1631  
1980

# ANALYSIS OF LIQUID VOLUME AND LIQUID MASS FRACTIONS AT COEXISTENCE FOR PURE FLUIDS

---

Lambert John Van Poolen, Ph. D.†

Thermophysical Properties Division  
National Engineering Laboratory  
National Bureau of Standards  
Boulder, Colorado 80303

May 1980

† Guest Worker: Professor of Engineering  
Calvin College  
Grand Rapids, Michigan 49506



---

U.S. DEPARTMENT OF COMMERCE, Philip M. Klutznick, Secretary

Luther H. Hodges, Jr., Deputy Secretary

Jordan J. Baruch, Assistant Secretary for Productivity, Technology and Innovation

NATIONAL BUREAU OF STANDARDS, Ernest Ambler, Director



## CONTENTS

	Page
1. INTRODUCTION . . . . .	1
2. MATHEMATICAL DESCRIPTION OF $X_{LV}$ AND $X_{LM}$ . . . . .	2
3. ANALYSIS OF $X_{LV}$ AND $X_{LM}$ . . . . .	4
3.1 Maxima and Minima Analysis for $T_{TP} < T < T_C$ . . . . .	4
3.2 Maxima and Minima Analysis as T Goes to $T_C$ . . . . .	17
3.3 Analysis Along $\rho_c$ and $X_{C,LIM}$ as T Goes to $T_C$ . . . . .	22
3.4 Maxima and Minima Analysis as T Goes to $T_{TP}$ . . . . .	36
4. CORRELATING COEXISTENCE - CRITICAL POINT DATA USING THE LIQUID VOLUME FRACTION . . . . .	37
5. EXPERIMENTAL APPROACH TO SIMULTANEOUS DETERMINATION OF COEXISTENCE DATA . . . . .	51
6. SUMMARY . . . . .	55
7. ACKNOWLEDGMENTS . . . . .	55
8. REFERENCES . . . . .	56
APPENDIX A. Symbols and Units . . . . .	58

LIST OF FIGURES

	Page
Figure 1. $X_{LV}$ vs T for $CH_4$ at constant $\rho_T$ . . . . .	5
Figure 2. $X_{LM}$ vs T for $CH_4$ at constant $\rho_T$ . . . . .	6
Figure 3. $\rho_T$ vs T for $CH_4$ at constant $X_{LV}$ . . . . .	7
Figure 4. $\rho_T$ vs T for $CH_4$ at constant $X_{LM}$ . . . . .	8
Figure 5. $X_{LV}$ vs $\rho_T$ for $CH_4$ at constant T . . . . .	9
Figure 6. $X_{LM}$ vs $\rho_T$ for $CH_4$ at constant T . . . . .	10
Figure 7. Verification of $X_{LV} - X_{LM}$ structure . . . . .	15
Figure 8. $X_{LV,MAX}$ First Possibility . . . . .	23
Figure 9. $X_{LV,MAX}$ Second Possibility . . . . .	24
Figure 10. Data for $X_{LV,MAX}$ Possibility Analysis . . . . .	26
Figure 11. Implications of $X_{C,LIM} > 1/2$ . . . . .	34
Figure 12. Percent Deviation Plot of $\rho_\ell + \rho_v$ for Ethylene . . . . .	45
Figure 13. $3\sigma$ Confidence Limit Band on $\rho_\ell + \rho_v$ of Ethylene . . . . .	50
Figure 14. $X_{LV}$ vs $\rho_T$ to Find $\rho_\ell$ and $\rho_v$ for Ammonia . . . . .	52

LIST OF TABLES

Table 1. $X_{LV,C}$ and $X_{LV,MAX}$ for Ethylene . . . . .	27
Table 2. Effect of $\phi$ , $B_{1\ell}$ , and, $B_{1v}$ on $\lim_{T \rightarrow T_c} \left. \frac{\partial \rho_T}{\partial T} \right _{X_{LV}=X_{C,LIM}}$ and $\lim_{T \rightarrow T_c} (\rho'_\ell + \rho'_v)$ . . . . .	32
Table 3. Analysis of $(B_{2\ell} + B_{2v})$ for $(B_{1\ell} = -B_{1v})$ . . . . .	33
Table 4. Check on Inequalities for Ethylene . . . . .	36
Table 5. $X_{LV,C}$ vs T for Argon . . . . .	39
Table 6. $X_{LV,C}$ vs T for Ammonia . . . . .	40
Table 7. Experimental Ethylene Data . . . . .	42
Table 8. $X_{LV,C}$ and $(\rho_\ell + \rho_v)$ Comparison for Ethylene . . . . .	43
Table 9. Critical Properties of Ethylene . . . . .	46
Table 10. $\rho_\ell$ (mol/dm <sup>3</sup> ) Comparisons for Ethylene . . . . .	47
Table 11. $\rho_v$ (mol/dm <sup>3</sup> ) Comparisons for Ethylene . . . . .	47
Table 12. Comparison of Coexistence Densities (g/cm <sup>3</sup> ) . . . . .	53
Table 13. Comparison of $\rho_v$ Values (g/cm <sup>3</sup> ) . . . . .	54
Table 14. Comparison of $\rho_\ell$ Values (g/cm <sup>3</sup> ) . . . . .	54

ANALYSIS OF LIQUID VOLUME AND LIQUID MASS FRACTIONS AT  
COEXISTENCE FOR PURE FLUIDS

Lambert John Van Poolen

An analysis of the behavior of liquid volume and liquid mass fractions at coexistence for pure fluids is made. Scaled equations for the saturation liquid and vapor densities are analyzed and relationships between various exponents and among constant coefficients are presented. Inequalities which exist among the saturation densities and their derivatives are developed. A procedure to correlate saturation data with the critical point is applied to ethylene. An experimental procedure to determine, simultaneously, saturated liquid and vapor densities at a given temperature is presented.

Key words: Coexistence densities; critical density; critical point; liquid mass fraction; liquid volume fraction; phase equilibria; pure fluids.

1. INTRODUCTION

A complete description of a pure fluid at liquid-vapor coexistence from a P-V-T perspective is given by the intensive variables:

P, vapor pressure,

T, vapor temperature,

$\rho_\ell$ , saturated liquid density,

$\rho_v$ , saturated vapor density,

and the following extensive variables:

$m_\ell$ ,  $m_v$ , masses of the two phases ( $m_\ell + m_v = m_T = \text{total mass}$ ),

$V_\ell$ ,  $V_v$ , volumes of the two phases ( $V_\ell + V_v = V_T = \text{total volume}$ ).

Of the four intensive variables only one is independent, i.e., there is one degree of freedom as described by the Gibbs phase rule. For the purpose of this work, T is assumed the independent variable.

An analysis of the extensive variables reveals that any two are independent variables. Hence, to completely describe the pure fluid at coexistence it is sufficient to specify one intensive variable and two extensive variables, i.e., the overall system has three degrees of freedom.

It is not obvious that useful information about the coexistence state is to be gained by considering the extensive variables along with the intensive ones. However, an investigation of these extensive variables when normalized by the total volume and/or total mass has proven interesting.

Consider the mass balance at coexistence,

$$m_T = m_\ell + m_v, \quad (1)$$

normalized by  $V_T$ , utilizing the fact that

$$m_\ell = \rho_\ell V_\ell \text{ and } m_v = \rho_v V_v, \quad (2)$$

with the result that

$$(m_T/V_T) = \rho_\ell (V_\ell/V_T) + \rho_v (V_v/V_T) . \quad (3)$$

Now define:

$$\rho_T \equiv m_T/V_T, \text{ overall or total density,}$$

$$X_{LV} \equiv V_\ell/V_T, \text{ liquid volume fraction,}$$

and since

$$1 - X_{LV} \equiv V_v/V_T,$$

the overall density is

$$\rho_T = \rho_\ell X_{LV} + \rho_v (1 - X_{LV}) , \quad (4)$$

or rewriting,

$$X_{LV} = (\rho_T - \rho_v)/(\rho_\ell - \rho_v) . \quad (5)$$

Now,  $\rho_v = \rho_v(T)$  and  $\rho_\ell = \rho_\ell(T)$ , therefore, eq. (5) describes a variable field having two degrees of freedom - one from the intensive variable set ( $T$ ) and one from the extensive variable set ( $m_T/V_T = \rho_T$ ). Another extensive variable, perhaps  $V_T$ , would also have to be explicitly known to completely describe a system at coexistence. However, eq. (5) does provide a connection between the intensive and extensive variables and it is that connection,  $X_{LV}$ , which provides the interest.

The liquid mass fraction:

$$X_{LM} \equiv m_\ell/m_T$$

is found directly from the liquid volume fraction, i.e.,

$$X_{LM} \equiv m_\ell/m_T = (V_\ell \rho_\ell)/(V_T \rho_T) = (\rho_\ell/\rho_T) X_{LV} . \quad (6)$$

The two variable fields to be explored are then (from (5)):

$$f(X_{LV}, \rho_T, T) = 0, \text{ i.e., } X_{LV} = (\rho_T - \rho_v)/(\rho_\ell - \rho_v)$$

and from (6) and (5),

$$g(X_{LM}, \rho_T, T) = 0, \text{ i.e., } X_{LM} = (\rho_\ell/\rho_T)(\rho_T - \rho_v)/(\rho_\ell - \rho_v) . \quad (7)$$

## 2. MATHEMATICAL DESCRIPTION OF $X_{LV}$ AND $X_{LM}$

For  $f(X_{LV}, \rho_T, T) = 0$  we expect:

$$\left. \frac{\partial X_{LV}}{\partial T} \right|_{\rho_T} \left. \frac{\partial T}{\partial \rho_T} \right|_{X_{LV}} \left. \frac{\partial \rho_T}{\partial X_{LV}} \right|_T = -1 \quad (8)$$

and from eq. (5) the derivatives are:

$$\left. \frac{\partial X_{LV}}{\partial T} \right|_{\rho_T} = \frac{-\rho_V'}{(\rho_L - \rho_V)} - X_{LV} \frac{(\rho_L' - \rho_V')}{(\rho_L - \rho_V)} \quad (9)$$

$$\left. \frac{\partial X_{LV}}{\partial \rho_T} \right|_T = \frac{1}{(\rho_L - \rho_V)} \quad (10)$$

$$\left. \frac{\partial \rho_T}{\partial T} \right|_{X_{LV}} = \rho_V' + X_{LV}(\rho_L' - \rho_V') \quad (11)$$

Indeed eqs. (9), (10), and (11) together satisfy eq. (8) - the chain rule. It can also be shown that for:

$$dX_{LV} = \left. \frac{\partial X_{LV}}{\partial \rho_T} \right|_T d\rho_T + \left. \frac{\partial X_{LV}}{\partial T} \right|_{\rho_T} dT \quad (12)$$

that:

$$\frac{\partial^2 X_{LV}}{\partial T \partial \rho_T} = \frac{\partial^2 X_{LV}}{\partial \rho_T \partial T}$$

indicating that  $dX_{LV}$  is an exact differential and that  $X_{LV}$  is a thermodynamic property.

For  $g(X_{LM}, \rho_T, T) = 0$  we have:

$$\left. \frac{\partial X_{LM}}{\partial T} \right|_{\rho_T} \left. \frac{\partial T}{\partial \rho_T} \right|_{X_{LM}} \left. \frac{\partial \rho_T}{\partial X_{LM}} \right|_T = -1 \quad (13)$$

and from eq. (7) the derivatives are:

$$\left. \frac{\partial X_{LM}}{\partial T} \right|_{\rho_T} = \frac{-\rho_L \rho_V'}{\rho_T(\rho_L - \rho_V)} + X_{LM} \frac{(\rho_L \rho_V' - \rho_L' \rho_V)}{\rho_L(\rho_L - \rho_V)} \quad (14)$$

$$\left. \frac{\partial X_{LM}}{\partial \rho_T} \right|_T = \frac{\rho_V \rho_L}{\rho_T^2 (\rho_L - \rho_V)} \quad (15)$$

$$\left. \frac{\partial \rho_T}{\partial T} \right|_{X_{LM}} = \frac{\rho_T \rho_V'}{\rho_V} - \frac{X_{LM} \rho_T^2 (\rho_L \rho_V' - \rho_L' \rho_V)}{\rho_L^2 \rho_V} \quad (16)$$

Indeed eqs. (14), (15), and (16) satisfy eq. (13). It can also be shown that for:

$$dX_{LM} = \left. \frac{\partial X_{LM}}{\partial \rho_T} \right|_T d\rho_T + \left. \frac{\partial X_{LM}}{\partial T} \right|_{\rho_T} dT \quad (17)$$

that:

$$\frac{\partial^2 X_{LM}}{\partial T \partial \rho_T} = \frac{\partial^2 X_{LM}}{\partial \rho_T \partial T}$$

indicating that  $dX_{LM}$  is an exact differential and that  $X_{LM}$  is a thermodynamic property.

### 3. ANALYSIS OF $X_{LV}$ AND $X_{LM}$

#### 3.1 Maxima and Minima Analysis for $T_{TP} < T < T_C$

The fields  $f(X_{LV}, \rho_T, T) = 0$ , and  $g(X_{LM}, \rho_T, T) = 0$ , are plotted from smoothed methane data presented by IUPAC [1]. The results are shown in figs. 1-6.

For the maximum in  $X_{LV}$ , shown in fig. 1, eq. (9) can be set to zero, i.e.,

$$\left. \frac{\partial X_{LV}}{\partial T} \right|_{\rho_T} = \frac{-\rho'_V}{\rho_\ell - \rho_V} - X_{LV} \frac{(\rho'_\ell - \rho'_V)}{(\rho_\ell - \rho_V)} = 0 \quad .$$

Designating the subscript "MAX" for the point where the maximum occurs,

$$X_{LV,MAX} = \frac{-\rho'_V}{(\rho'_\ell - \rho'_V)} \quad \text{for } (\rho_\ell - \rho_V) \neq 0 \quad . \quad (18)$$

Now there is a corresponding  $\rho_{T,MAX}$  such that:

$$X_{LV,MAX} = (\rho_{T,MAX} - \rho_V) / (\rho_\ell - \rho_V)$$

or,

$$\rho_{T,MAX} = \frac{-\rho'_V}{(\rho'_\ell - \rho'_V)} (\rho_\ell - \rho_V) + \rho_V = \frac{(\rho_V \rho'_\ell - \rho'_V \rho_\ell)}{(\rho'_\ell - \rho'_V)} \quad . \quad (19)$$

Later on (see figs. 8, 9, and 10), when dealing directly with the critical liquid volume fraction,  $X_{LV,c}$  ( $\rho_T = \rho_c$ ), it is shown that it is unlikely that a maximum occurs along the curve describing it for  $T < T_C$ . The implication is that if a maximum does occur, the  $X_{LV}$  curve is turning towards zero and hence the  $\rho_T$  is a  $\rho_V$  (refer to fig. 1).

We can then conclude that  $\rho_{T,MAX} = \rho_V < \rho_c$  and hence:

$$X_{LV,c} > X_{LV,MAX} \quad . \quad (20)$$



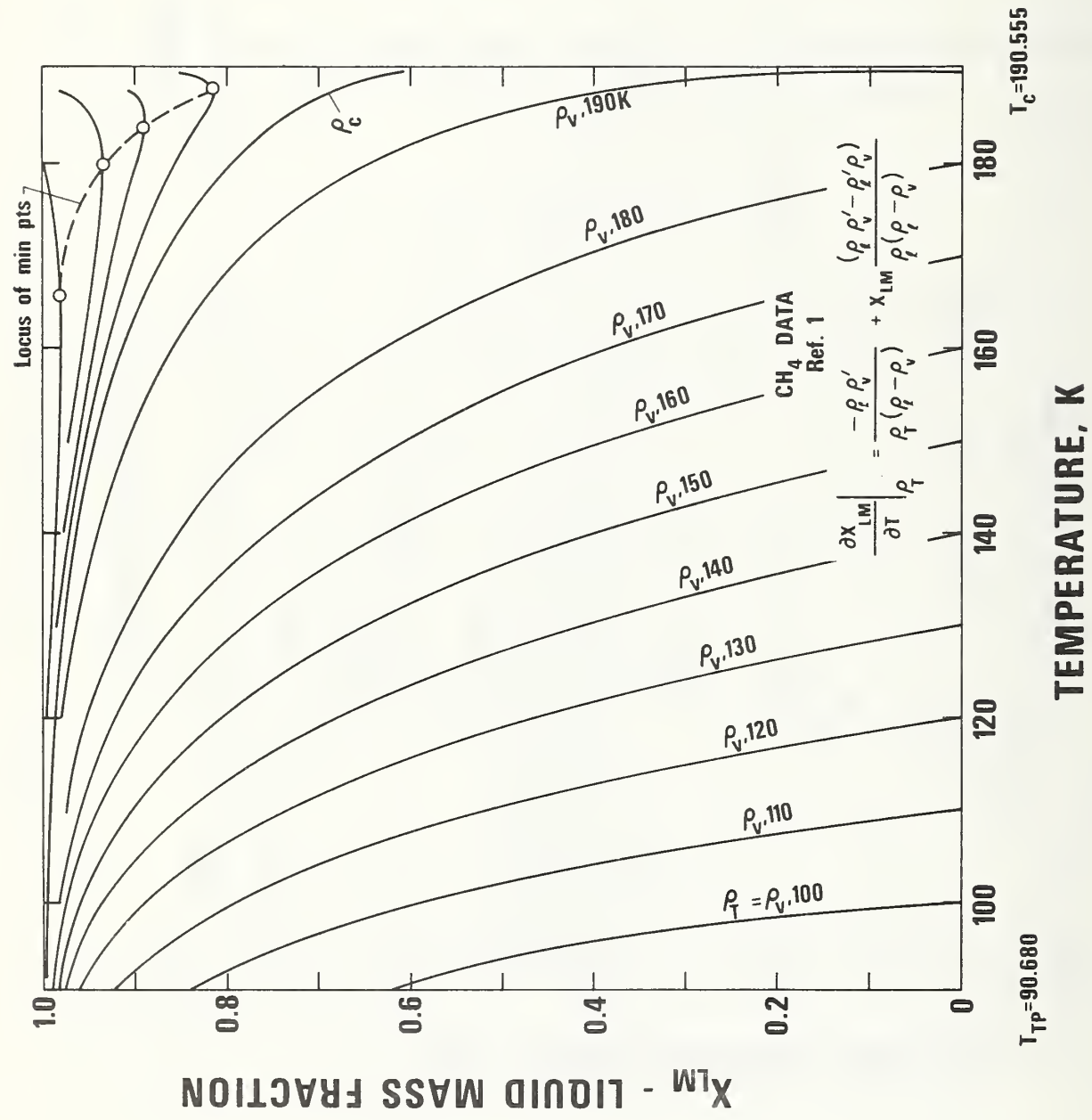


Figure 2.  $x_{LM}$  vs T for CH<sub>4</sub> at constant  $p_T$ .

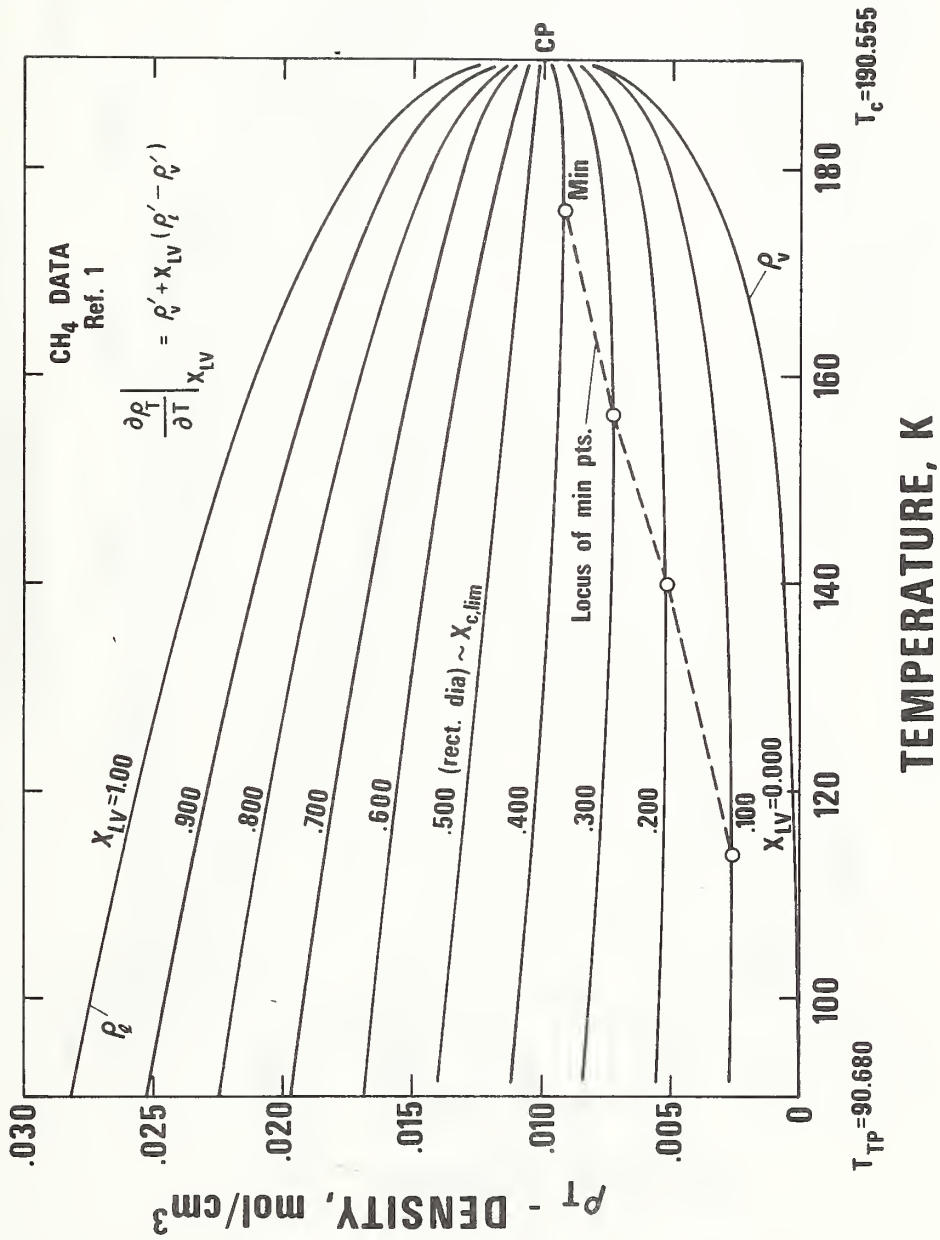


Figure 3.  $\rho_T$  vs  $T$  for CH<sub>4</sub> at constant  $X_{LV}$ .



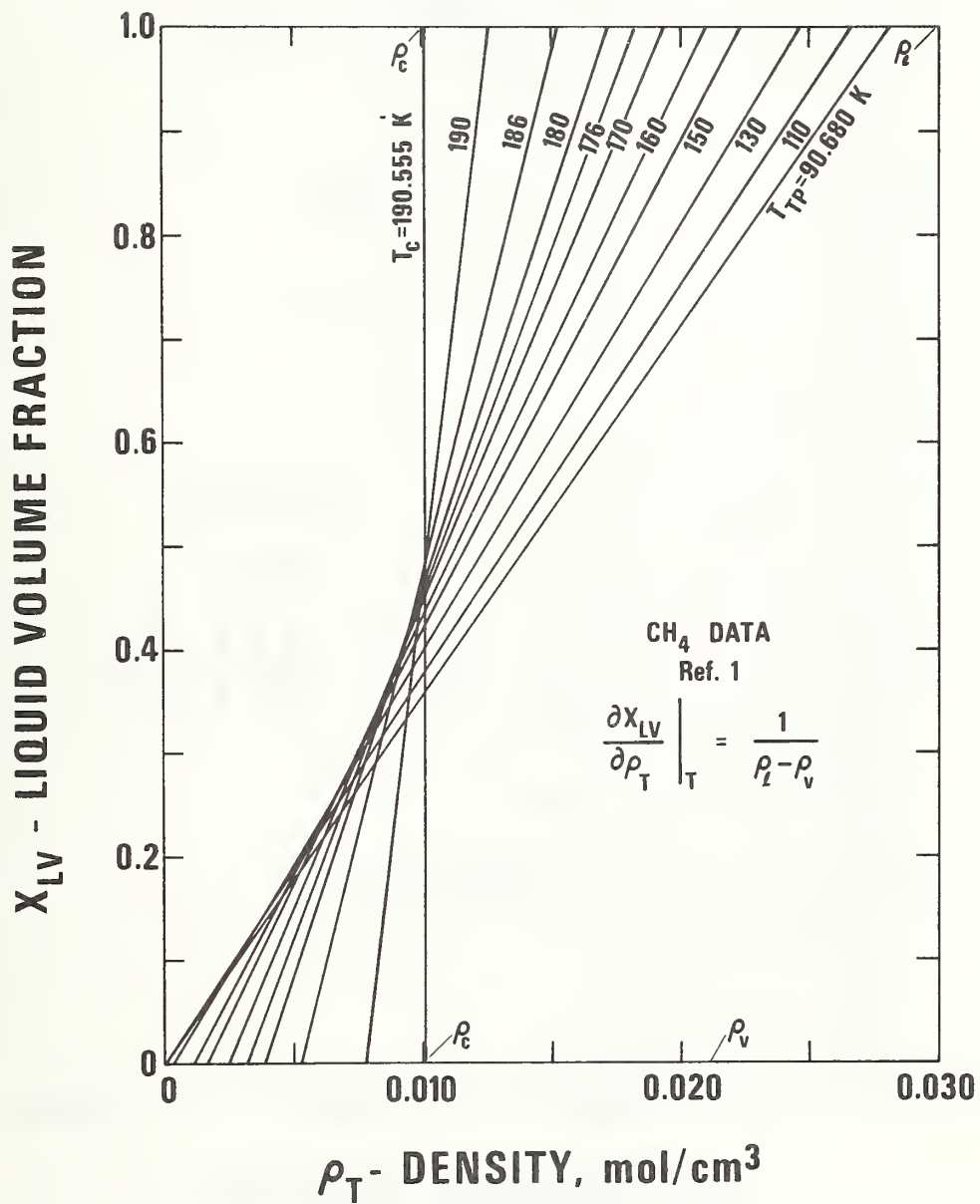


Figure 5.  $X_{LV}$  vs  $\rho_T$  for  $\text{CH}_4$  at constant  $T$ .

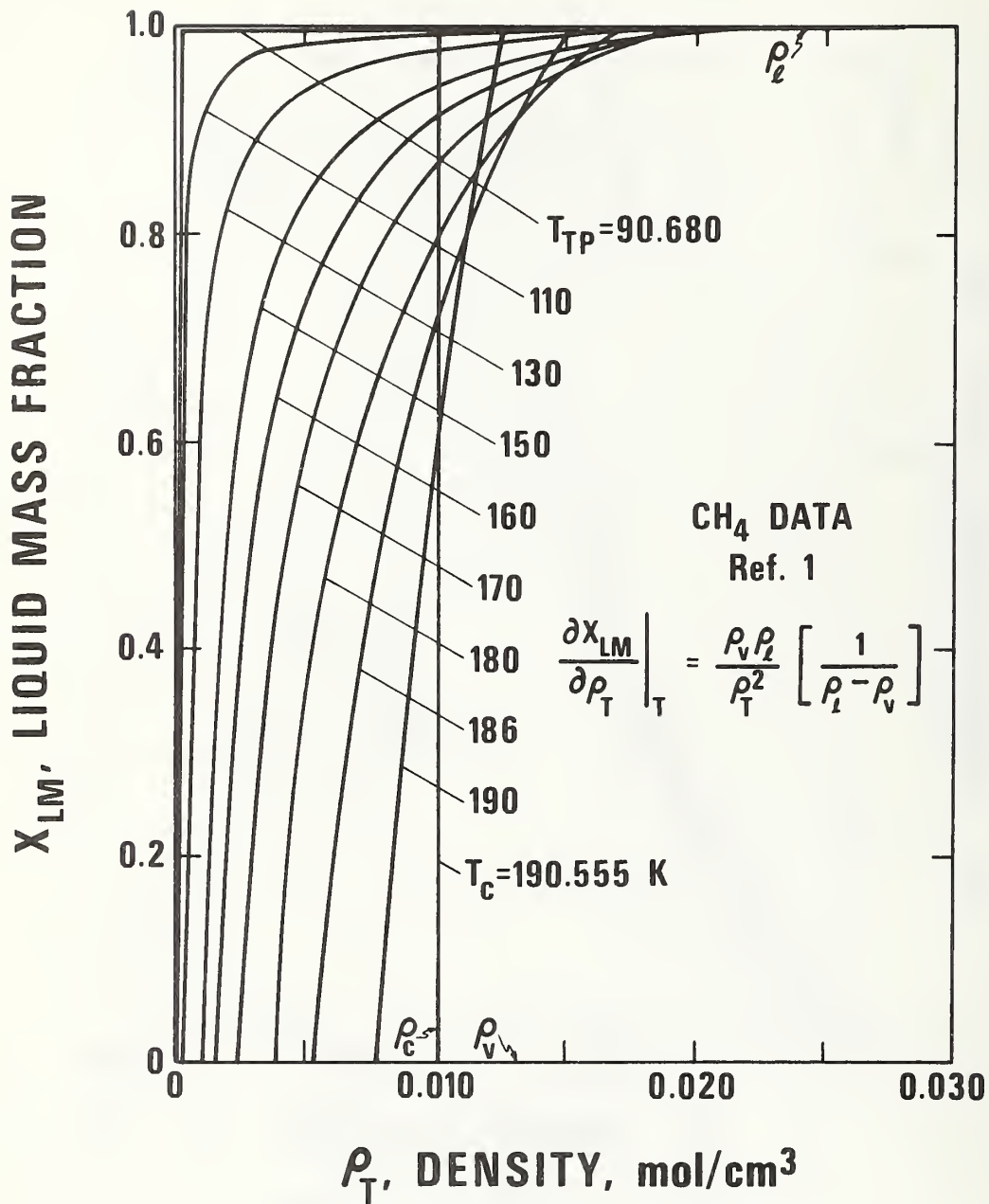


Figure 6.  $X_{LM}$  vs  $\rho_T$  for CH<sub>4</sub> at constant T.

The tendency towards zero for the  $\rho_T = \rho_V$  curves (or towards one for  $\rho_T = \rho_\ell$ ) is literally true in the absence of gravity effects. Indeed Hohenberg, et al. [2] indicate that within a very narrow range of temperature and overall density near the critical the meniscus, under the effect of gravity, disappears somewhere other than at the top or bottom of the test cell.

For the minimum in  $X_{LM}$ , shown in fig. 2, eq. (14) can be set to zero, i.e.,

$$\left. \frac{\partial X_{LM}}{\partial T} \right|_{\rho_T} = \frac{-\rho_\ell \rho_V'}{\rho_T(\rho_\ell - \rho_V)} + X_{LM} \frac{(\rho_\ell \rho_V' - \rho_\ell' \rho_V)}{\rho_\ell(\rho_\ell - \rho_V)} = 0 .$$

Using the subscript "MIN" for the point where the minimum occurs,

$$X_{LM,MIN} = \frac{\rho_\ell}{\rho_{T,MIN}} \left[ \frac{(\rho_\ell \rho_V')}{(\rho_\ell \rho_V' - \rho_\ell' \rho_V)} \right] . \quad (21)$$

Now the corresponding  $\rho_{T,MIN}$  is that for which

$$X_{LM,MIN} = \frac{\rho_\ell}{\rho_{T,MIN}} \left[ \frac{(\rho_{T,MIN} - \rho_V)}{(\rho_\ell - \rho_V)} \right] ,$$

or,

$$\rho_{T,MIN} = \frac{\rho_\ell \rho_V'}{(\rho_\ell \rho_V' - \rho_\ell' \rho_V)} (\rho_\ell - \rho_V) + \rho_V = (\rho_V' \rho_\ell^2 - \rho_\ell' \rho_V^2) / (\rho_\ell \rho_V' - \rho_\ell' \rho_V) . \quad (22)$$

In an argument similar to that for  $X_{LV,c} > X_{LV,MAX}$  it can be shown, based on fig. 2, that values of  $\rho_{T,MIN}$  are  $\rho_\ell$ 's and hence:

$$X_{LM,MIN} > X_{LM,c} , \quad (23)$$

where  $X_{LM,c}$  is the critical liquid mass fraction ( $\rho_T = \rho_c$ ).

If  $\rho_c$  is substituted for  $\rho_T$  in eqs. (5) and (7), the critical liquid volume fraction and critical liquid mass fraction are explicitly:

$$X_{LV,c} = (\rho_c - \rho_V) / (\rho_\ell - \rho_V) \quad (24)$$

$$X_{LM,c} = (\rho_\ell / \rho_c) (\rho_c - \rho_V) / (\rho_\ell - \rho_V) \quad (25)$$

Now,  $X_{LM,c} > X_{LV,c}$  at a given temperature by inspection of eqs. (24) and (25) since,

$\rho_\ell > \rho_c$ , therefore:

$$X_{LM,MIN} > X_{LM,c} > X_{LV,c} > X_{LV,MAX} \quad (26)$$

and

$$\rho_{T,MIN} > \rho_c > \rho_{T,MAX} \quad , \quad (27)$$

where  $\rho_l > \rho_c > \rho_v$ .

Also, considering the value of  $X_{LM}$  at the temperature and  $\rho_{T,MAX}$  for which  $X_{LV}$  is a maximum, i.e.,

$$X_{LM,MAX} = \frac{\rho_l}{\rho_{T,MAX}} X_{LV,MAX} \quad (\text{form of eq. 6})$$

Substituting for  $\rho_{T,MAX}$  eq. (19) and for  $X_{LV,MAX}$  eq. (18) the result is:

$$X_{LM,MAX} = \frac{\rho_l \rho'_v}{(\rho_l \rho'_v - \rho'_l \rho_v)} \quad . \quad (28)$$

Also, consider the value of  $X_{LV}$  at the temperature and  $\rho_{T,MIN}$  for which  $X_{LM}$  is a minimum, i.e.,

$$X_{LV,MIN} = \frac{\rho_{T,MIN}}{\rho_l} X_{LM,MIN} \quad (\text{form of eq. 6})$$

Substitute for  $\rho_{T,MIN}$  eq. (22) and for  $X_{LM,MIN}$  eq. (21) to obtain

$$X_{LV,MIN} = \frac{\rho_l \rho'_v}{\rho_l \rho'_v - \rho'_l \rho_v} \quad , \quad (29)$$

which is the same as  $X_{LM,MAX}$  for the same temperature (see eq. (28)). Now  $X_{LV,MIN}$  is the liquid volume fraction at a density  $\rho_l = \rho_{T,MIN} > \rho_c$ . Therefore:

$$X_{LV,MIN} > X_{LV,c} \quad (30)$$

and  $X_{LM,MAX}$  is the liquid mass fraction at a density  $\rho_v = \rho_{T,MAX} < \rho_c$  so

$$X_{LM,MAX} < X_{LM,c} \quad . \quad (31)$$

Combining eqs. (26), (28), (29), (30), and (31) results in:

$$X_{LM,MIN} > X_{LM,c} > X_{LM,MAX} = X_{LV,MIN} > X_{LV,c} > X_{LV,MAX} \quad . \quad (32)$$

An investigation of the individual terms in eq. (32) and their related equations indicates they are only functions of temperature. This is interesting since the field describing the coexistence states has two degrees of freedom. Therefore, these are loci of points, having only one degree of freedom. This reduction comes via the "zero" condition on the first derivative. Also, some conclusions can be drawn about the derivatives,

$$\left. \frac{\partial X_{LM}}{\partial T} \right|_{\rho_{T,MAX}} \quad \text{and} \quad \left. \frac{\partial X_{LV}}{\partial T} \right|_{\rho_{T,MIN}}, \quad \text{at the same temperature.}$$

From eq. (6),

$$\left. \frac{\partial X_{LM}}{\partial T} \right|_{\rho_T} = \frac{1}{\rho_T} \left[ \rho_\ell \left. \frac{\partial X_{LV}}{\partial T} \right|_{\rho_T} + \rho_\ell' X_{LV} \right] \quad (33)$$

Now at a minimum,  $\left. \frac{\partial X_{LM}}{\partial T} \right|_{\rho_T} = 0$  and from eq. (33),

$$\rho_\ell \left. \frac{\partial X_{LV}}{\partial T} \right|_{\rho_{T,MIN}} + \rho_\ell' X_{LV,MIN} = 0, \quad (34)$$

and from,

$$X_{LV} = \frac{\rho_T}{\rho_\ell} X_{LM}, \quad (\text{form of eq. 6})$$

obtain:

$$\left. \frac{\partial X_{LV}}{\partial T} \right|_{\rho_T} = \rho_T \left[ \frac{1}{\rho_\ell} \left. \frac{\partial X_{LM}}{\partial T} \right|_{\rho_T} - \frac{X_{LM} \rho_\ell'}{\rho_\ell^2} \right]. \quad (35)$$

At a maximum,  $\left. \frac{\partial X_{LV}}{\partial T} \right|_{\rho_T} = 0$ , therefore from eq. (35):

$$\rho_\ell \left. \frac{\partial X_{LM}}{\partial T} \right|_{\rho_{T,MAX}} - X_{LM,MAX} \rho_\ell' = 0. \quad (36)$$

Combining eqs. (34) and (36):

$$\frac{X_{LV,MIN}}{X_{LM,MAX}} = - \frac{\left. \frac{\partial X_{LV}}{\partial T} \right|_{\rho_{T,MIN}}}{\left. \frac{\partial X_{LM}}{\partial T} \right|_{\rho_{T,MAX}}} \quad (37)$$

and as previously shown from eqs. (28) and (29):

$$X_{LV,MIN} = X_{LM,MAX}, \quad (38)$$

therefore:

$$\left. \frac{\partial X_{LV}}{\partial T} \right|_{\rho_{T,MIN}} = - \left. \frac{\partial X_{LM}}{\partial T} \right|_{\rho_{T,MAX}}. \quad (39)$$

The methane data of IUPAC [1] was analyzed to check the validity of eqs. (27), (32), (38), and (39). The results are shown in fig. 7 for one temperature, 344 K (160°F). The data used is published at two degree intervals and the slight errors in the equality of  $X_{LM,MAX}$

to  $X_{LV,MIN}$  and  $\left. \frac{\partial X_{LV}}{\partial T} \right|_{\rho_{T,MIN}}$  to  $-\left. \frac{\partial X_{LM}}{\partial T} \right|_{\rho_{T,MAX}}$  reflect the effect of using this large temperature increment in the numerical calculation of the derivatives.

An examination of fig. 3 reveals a minimum in  $\rho_T$  versus T at constant  $X_{LV} < X_{C,LIM}$  (limit of critical liquid volume fraction).

Substituting eq. (5) into eq. (11) and setting the derivative to zero,

$$\left. \frac{\partial \rho_T}{\partial T} \right|_{X_{LV}} = 0 = \rho'_V + \frac{(\rho_T - \rho_V)}{(\rho'_L - \rho'_V)} (\rho'_L - \rho'_V) ,$$

the expression for  $\rho_T$  at the minimum is:

$$\rho_{T,ZERO \text{ SLOPE}} = \frac{\rho_V \rho'_L - \rho'_V \rho_L}{(\rho'_L - \rho'_V)} ,$$

which is the same as eq. (19). Thus these minimums in fig. 3 correspond to the maximums in fig. 1.

A similar analysis of the maximums in fig. 4 reveal that they correspond to the minimums in fig. 2.

An interesting inequality arises from the fact that the second derivative of  $X_{LV}$  at the maximum shown in fig. 1 must be less than zero. The derivative of eq. (9) is calculated recognizing that at the point of consideration:

$$\left. \frac{\partial X_{LV}}{\partial T} \right|_{\rho_{T,MAX}} = 0 \text{ by definition, and } X_{LV,MAX} \text{ is given by eq. (18),}$$

with the result:

$$\left. \frac{\partial^2 X_{LV}}{\partial T^2} \right|_{\rho_{T,MAX}} = \frac{(\rho'_V \rho''_L) + (-\rho''_V \rho'_L)}{(\rho'_L - \rho'_V)(\rho_L - \rho_V)} \quad (40)$$

Now by inspection of figs. 3 or 4,

$$\begin{aligned} \rho'_V > 0 \quad , \quad \rho'_L < 0 \\ \rho''_V > 0 \quad , \quad \rho''_L < 0 \quad . \end{aligned} \quad (41)$$

In terms of signs, eq. (40) is:

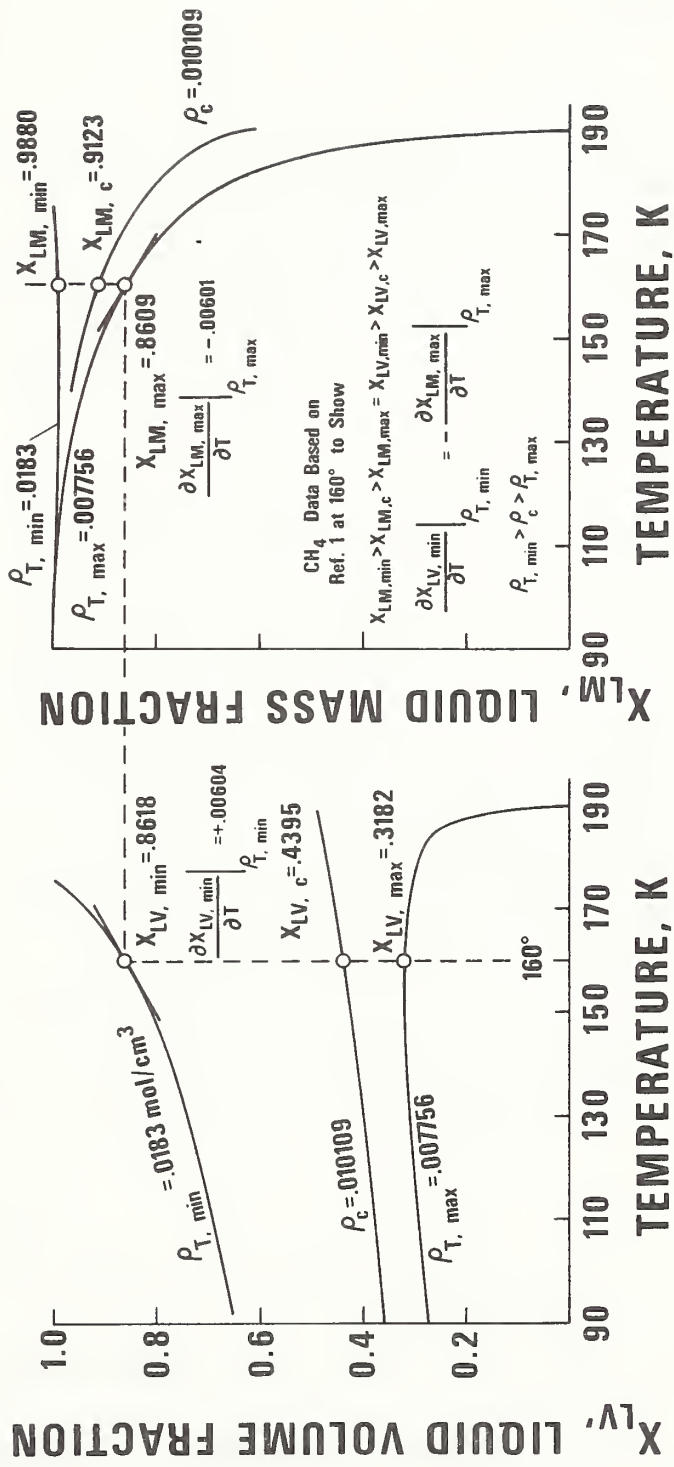


Figure 7. Verification of  $X_{LV} - X_{LM}$  structure.

$$\left. \frac{\partial^2 X_{LV}}{\partial T^2} \right|_{\rho_{T,MAX}} = \frac{(-) + (+)}{(-)(+)} .$$

Therefore if  $\left. \frac{\partial^2 X_{LV}}{\partial T^2} \right|_{\rho_{T,MAX}}$  is to be less than zero,

$$\left| \rho_V'' \rho_\ell' \right| > \left| \rho_\ell'' \rho_V' \right| \quad (42)$$

This same conclusion can be reached from the minimums in fig. 3. From the derivative of eq. (16),

$$\left. \frac{\partial^2 \rho_T}{\partial T^2} \right|_{X_{LV}} = \rho_V'' + \left. \frac{\partial X_{LV}}{\partial T} \right|_{\rho_T} (\rho_\ell' - \rho_V') + X_{LV} (\rho_\ell'' - \rho_V'') \quad (43)$$

Now, as seen in an earlier analysis, at this minimum:

$$\left. \frac{\partial X_{LV}}{\partial T} \right|_{\rho_T} = 0 ,$$

and:

$$X_{LV} = X_{LV,MAX} = - \rho_V' / (\rho_\ell' - \rho_V') \quad (44)$$

After substitution of these in eq. (43):

$$\left. \frac{\partial^2 \rho_T}{\partial T^2} \right|_{X_{LV,MAX}} = \frac{(\rho_V'' \rho_\ell') + (-\rho_V' \rho_\ell'')}{(\rho_\ell' - \rho_V')(\rho_\ell' - \rho_V')} \quad (44)$$

If this is a true minimum  $\left. \frac{\partial^2 \rho_T}{\partial T^2} \right|_{X_{LV,MAX}}$  should be greater than zero. This is true if

again:

$$\left| \rho_V'' \rho_\ell' \right| > \left| \rho_\ell'' \rho_V' \right| \quad (42)$$

And since we have already indicated that a maximum in  $X_{LV}$  exists for all  $T_{TP} < T < T_C$ , eq. (42) is true for this temperature range.

Consider the minimum in  $X_{LM}$  as seen in fig. 2. The related derivative is given by eq. (14).

If the minimum is truly so, the curve is concave upward and the second derivative is positive at that point.

We had at this minimum,  $\left. \frac{\partial X_{LM}}{\partial T} \right|_{\rho_{T,MIN}} = 0$ , and from previous work eqs. (21) and (22)

apply.

Taking the derivative of eq. (14) and substituting eqs. (21) and (22) the result is:

$$\left. \frac{\partial^2 X_{LM}}{\partial T^2} \right|_{\rho_{T,MIN}} = \frac{(-\rho_V \rho_L \rho_L'' \rho_V' + 2\rho_V' \rho_L' (\rho_L' \rho_V - \rho_V' \rho_L)) + (\rho_V \rho_L \rho_V'' \rho_L')}{(\rho_L - \rho_V)(\rho_V' \rho_L^2 - \rho_L' \rho_V^2)} \quad (45)$$

Equation (45) in terms of signs using eq. (41) is:

$$\left. \frac{\partial^2 X_{LM}}{\partial T^2} \right|_{\rho_{T,MIN}} = \frac{(+)+(-)}{(+)(+)} .$$

If  $\left. \frac{\partial^2 X_{LM}}{\partial T^2} \right|_{\rho_{T,MIN}}$  is to be greater than zero,

$$\left| -\rho_V \rho_L \rho_L'' \rho_V' + 2\rho_V' \rho_L' (\rho_L' \rho_V - \rho_V' \rho_L) \right| > \left| \rho_V \rho_L \rho_V'' \rho_L' \right| . \quad (46)$$

This is true for  $T_{TP} < T < T_C$  for which a minimum in  $X_{LM}$  occurs. (No doubt eq. (46) can also be found by considering the maximum in fig. 4. This was not done.)

### 3.2 Maxima and Minima Analysis as T Goes to $T_C$

To aid in this limit analysis, use is made of the following coexistence dome equations based on those given by Green, et al. [3], and Sengers, et al. [4] with the exception that the exponents are not assumed the same for each phase, i.e.,

$$\rho_L - \rho_C = B_{1L} \epsilon^{\beta_L} + B_{2L} \epsilon^{\phi_L} + B_{3L} \epsilon^{\psi_L} \quad (47)$$

$$\rho_V - \rho_C = B_{1V} \epsilon^{\beta_V} + B_{2V} \epsilon^{\phi_V} + B_{3V} \epsilon^{\psi_V} \quad (48)$$

where,

B's are constants,

$$\beta_L, \beta_V \cong .35$$

$$\phi_L, \phi_V \cong 1.00$$

$$\psi_L, \psi_V > 1.00$$

$$\epsilon = T_C - T.$$

To analyze the limits of various mass and liquid fractions in eq. (32) it is helpful to develop the relationship between the exponents  $\beta_V$  and  $\beta_L$  in eqs. (47) and (48).

To that end, form the critical liquid volume fraction  $X_{LV,c} = (\rho_c - \rho_v)/(\rho_\ell - \rho_v)$  using eqs. (47) and (48), i.e.:

$$X_{LV,c} = \frac{-B_{1V}\epsilon^{\beta_V - B_{2V}\epsilon^{\phi_V} - B_{3V}\epsilon^{\psi_V}}}{B_{1\ell}\epsilon^{\beta_\ell - B_{1V}\epsilon^{\beta_V}} + B_{2\ell}\epsilon^{\phi_\ell - B_{2V}\epsilon^{\phi_V}} + B_{3\ell}\epsilon^{\psi_\ell - B_{3V}\epsilon^{\psi_V}}} \quad (49)$$

Now fig. 1 indicates the generally accepted fact that the liquid volume fraction in the limit along the critical isochore is neither one (a liquid) nor zero (a vapor). A recent detailed critical point investigation by Moldover [5] reinforces such an opinion.

With that in mind, it may be assumed in eq. (49) that  $\beta_\ell > \beta_V$ , and each term can be divided by  $\epsilon^{\beta_V}$  obtaining:

$$X_{LV,c} = \frac{-B_{1V} + \text{TERMS}(\epsilon^{\text{EXP}>0})}{-B_{1V} + \text{TERMS}(\epsilon^{\text{EXP}>0})} \quad (50)$$

where "EXP" means the exponent of  $\epsilon$ . In the limit as  $T \rightarrow T_c$  ( $\epsilon \rightarrow 0$ )

$$\lim_{T \rightarrow T_c} X_{LV,c} = 1 \quad \text{for } \beta_\ell > \beta_V \quad (51)$$

Or if it is assumed that,  $\beta_V > \beta_\ell$ , and each term of eq. (49) is divided by  $\epsilon^{\beta_\ell}$  the result is:

$$X_{LV,c} = \frac{\text{TERMS}(\epsilon^{\text{EXP}>0})}{B_{1\ell} + \text{TERMS}(\epsilon^{\text{EXP}>0})} \quad (52)$$

In the limit then as  $T \rightarrow T_c$  ( $\epsilon \rightarrow 0$ )

$$\lim_{T \rightarrow T_c} X_{LV,c} = 0 \quad \text{for } \beta_V > \beta_\ell \quad (53)$$

Neither of these conclusions, eqs. (51) and (53), agree with the accepted fact that

$$0 < \lim_{T \rightarrow T_c} X_{LV,c} < 1 \quad (54)$$

The only possible conclusion is:

$$\beta_\ell = \beta_V \equiv \beta \quad (55)$$

In most of the current work with eqs. (47) and (48) the " $\beta$  exponents" are assumed equal. However, the behavior of the critical liquid volume fraction gives a rational reason for their equality. If this is true each term of eq. (49) can be divided by  $\epsilon^\beta$  obtaining,

$$X_{LV,c} = \frac{-B_{1V} + \text{TERMS}(\epsilon^{\text{EXP}>0})}{(B_{1l} - B_{1V}) + \text{TERMS}(\epsilon^{\text{EXP}>0})} \cdot \quad (62)$$

In the limit, then, as  $T \rightarrow T_c$  ( $\epsilon \rightarrow 0$ ):

$$\lim_{T \rightarrow T_c} X_{LV,c} = \frac{-B_{1V}}{B_{1l} - B_{1V}} \equiv X_{c,LIM} \cdot \quad (63)$$

We note that obviously  $B_{1V}$  nor  $B_{1l}$  is zero leading again to limits of zero and one respectively. Also, Sengers, et al. [4] indicate that for first order "dome" symmetry at the critical point,

$$B_{1l} = -B_{1V} \cdot \quad (64)$$

indicating also (see eq. (63)) that  $B_{1l}$  and  $B_{1V}$  are of opposite algebraic sign. Normally  $B_{1l}$  is positive while  $B_{1V}$  is negative (see eqs. (47) and (48)).

Also, the limit,  $T \rightarrow T_c$ , in eq. (6), i.e.,

$$\lim_{T \rightarrow T_c} X_{LM,c} = \lim_{T \rightarrow T_c} \frac{\rho_l}{\rho_c} \lim_{T \rightarrow T_c} X_{LV,c}$$

results in:

$$\lim_{T \rightarrow T_c} X_{LM,c} = \lim_{T \rightarrow T_c} X_{LV,c} = X_{c,LIM} \cdot \quad (65)$$

The critical isochores in figs. 1 and 2 can then be extended to the point "X" =  $-B_{1V}/(B_{1l} - B_{1V})$ , i.e., to  $X_{c,LIM}$  at  $T_c = 190.555$  K for the methane.

The limits of the liquid mass and volume fractions found in eq. (32) can be analyzed. Substituting the derivatives of eqs. (47) and (48) into eq. (18) and dividing each term by,  $\epsilon^{\beta-1}$ ,

$$X_{LV,MAX} = \frac{-\beta B_{1V} + \text{TERMS}(\epsilon^{\text{EXP}>0})}{+\beta (B_{1l} - B_{1V}) + \text{TERMS}(\epsilon^{\text{EXP}>0})} \cdot \quad (66)$$

In the limit ( $\epsilon \rightarrow 0$ ):

$$\lim_{T \rightarrow T_c} X_{LV,MAX} = \frac{-B_{1V}}{(B_{1l} - B_{1V})} = X_{c,LIM} \quad (67)$$

and for eq. (21), in the limit ( $\epsilon \rightarrow 0$ ), by inspection,

$$\lim_{T \rightarrow T_c} X_{LM,MIN} = \lim_{T \rightarrow T_c} X_{LV,MAX} = X_{c,LIM} \cdot \quad (68)$$

The results given in eqs. (67) and (68) allow the extension of the locus of maximum and minimum points to  $X_{c,LIM}$  at  $T_c$  on the figs. 1 and 2 and to  $\rho_c$  on figs. 3 and 4 at  $T_c$ .

Examining  $X_{LV,MIN}$  and  $X_{LM,MAX}$  in the context of eq. (38) it can be seen by inspection that as  $T \rightarrow T_c$ ,

$$\lim_{T \rightarrow T_c} X_{LV,MIN} = \lim_{T \rightarrow T_c} X_{LM,MAX} = \lim_{T \rightarrow T_c} X_{LV,MAX} = X_{c,LIM} \quad (69)$$

Thus eq. (32) can be rewritten for the limit at the critical as:

$$\begin{aligned} \lim_{T \rightarrow T_c} X_{LM,MIN} &= \lim_{T \rightarrow T_c} X_{LM,c} = \lim_{T \rightarrow T_c} X_{LM,MAX} = \lim_{T \rightarrow T_c} X_{LV,MIN} \\ &= \lim_{T \rightarrow T_c} X_{LV,c} = \lim_{T \rightarrow T_c} X_{LV,MAX} = X_{c,LIM} \end{aligned} \quad (70)$$

Since all these "X's" collapse to a single value at the critical point it might be expected that the derivatives of these curves at the points in eq. (32) would also go to a single value in the limit.

By inspection of figs. 1 and 2 and considering eq. (68) it is concluded that:

$$\lim_{T \rightarrow T_c} \left. \frac{\partial X_{LV}}{\partial T} \right|_{\rho_T = \rho_{T,MAX}} = 0 \quad (71)$$

and

$$\lim_{T \rightarrow T_c} \left. \frac{\partial X_{LM}}{\partial T} \right|_{\rho_T = \rho_{T,MIN}} = 0 \quad (72)$$

Further, consideration of eq. (69) suggests that the following limits also be considered:

$$\lim_{T \rightarrow T_c} \left. \frac{\partial X_{LV}}{\partial T} \right|_{\rho_T = \rho_{T,MIN}} \quad \text{and} \quad \lim_{T \rightarrow T_c} \left. \frac{\partial X_{LM}}{\partial T} \right|_{\rho_T = \rho_{T,MAX}}$$

The values of these derivatives can be found by combining eqs. (18), (19), (28), (36) and (39), to obtain:

$$\left. \frac{\partial X_{LM}}{\partial T} \right|_{\rho_T = \rho_{T,MAX}} = - \left. \frac{\partial X_{LV}}{\partial T} \right|_{\rho_T = \rho_{T,MIN}} = \frac{-\rho'_L \rho'_V}{(\rho'_L \rho'_V - \rho'_V \rho'_L)} \quad (73)$$

Substituting the derivatives from eqs. (47) and (48) into eq. (73) and dividing each term by  $(-\beta\epsilon^{\beta-1})$  results in:

$$\left. \frac{\partial X_{LM}}{\partial T} \right|_{\rho_T = \rho_{T,MAX}} = - \left. \frac{\partial X_{LV}}{\partial T} \right|_{\rho_T = \rho_{T,MIN}} = \frac{\beta B_{1L} B_{1V} \epsilon^{\beta-1} + \text{TERMS}(\epsilon^{EXP>0})}{\rho_C (B_{1L} - B_{1V}) + \text{TERMS}(\epsilon^{EXP>0})} \quad (74)$$

Noting that,  $B_{1L} B_{1V} < 0$  and  $(B_{1L} - B_{1V}) > 0$ , in the limit  $(\epsilon \rightarrow 0)$ :

$$\lim_{\substack{T \rightarrow T_c \\ \rho_{T,MIN} \rightarrow \rho_c^+}} \left. \frac{\partial X_{LV}}{\partial T} \right|_{\rho_T = \rho_{T,MIN}} = + \infty \quad (75)$$

$$\lim_{\substack{T \rightarrow T_c \\ \rho_{T,MAX} \rightarrow \rho_c^-}} \left. \frac{\partial X_{LM}}{\partial T} \right|_{\rho_T = \rho_{T,MAX}} = - \infty \quad (76)$$

So rather than uniformity in the derivatives at the critical point eqs. (71), (72), (75) and (76) indicate different values depending on whether the approach to  $\rho_C$  is from "below" or "above" and whether the function is  $X_{LV}$  or  $X_{LM}$ . These results are sensible in light of figs. 1 and 2. Also, since the maxima and minima of figs. 3 and 4 are shown to extend to the critical point, the limits,

$$\lim_{\substack{T \rightarrow T_c \\ X_{LV} \rightarrow X_{C,LIM}^-}} \left. \frac{\partial \rho_T}{\partial T} \right|_{X_{LV} \text{ at } \rho_{T,MAX}} = 0 \quad (77)$$

$$\lim_{\substack{T \rightarrow T_c \\ X_{LM} \rightarrow X_{C,LIM}^+}} \left. \frac{\partial \rho_T}{\partial T} \right|_{X_{LM} \text{ at } \rho_{T,MIN}} = 0 \quad (78)$$

seem reasonable. Also by analogy to eqs. (75) and (76) as well as by inspection of figs. 3 and 4,

$$\lim_{\substack{T \rightarrow T_c \\ X_{LV} \rightarrow X_{C,LIM}^+}} \left. \frac{\partial \rho_T}{\partial T} \right|_{X_{LV} \text{ at } \rho_{T,MIN}} = - \infty \quad (79)$$

$$\lim_{\substack{T \rightarrow T_c \\ X_{LM} \rightarrow X_{C,LIM}^-}} \left. \frac{\partial \rho_T}{\partial T} \right|_{X_{LM} \text{ at } \rho_{T,MAX}} = + \infty \quad (80)$$

seem to be rational conclusions.

### 3.3 Analysis Along $\rho_c$ and $X_{c,LIM}$ as $T$ Goes to $T_c$

It appears that to obtain a derivative at the critical point, unambiguously, the approach to the critical point must be along the critical isochore in figs. 1 and 2 and along the line  $X_{c,LIM}$  in figs. 3 and 4. Furthermore, the  $X_{LV,c}$  function has been utilized by this author [6] to both check the internal consistency of coexistence data and critical density values and to predict  $\rho_c$  from saturation data. (These procedures are discussed further later in this report.) A knowledge of the derivative is an obvious help to these ends.

The ambiguity in the limit prompts reconsideration of the function map and the areas of applicability of eqs. (8) and (13), i.e., the chain rules.

Now  $f(X_{LV}, \rho_T, T) = 0$ , becomes, along the critical isochore,  $f_c(X_{LM,c}, T) = 0$ .

Likewise  $g(X_{LM}, \rho_T, T) = 0$  becomes  $g_c(X_{LM,c}, T) = 0$ . This reduction in dependent variables is also true on the saturation boundaries, i.e.,  $f(X_{LV}, \rho_T, T) = f_\ell(\rho_\ell, T) = 0$  for  $X_{LV} = 1$ , and  $f(X_{LV}, \rho_T, T) = f_v(\rho_v, T) = 0$  for  $X_{LV} = 0$ . This would occur also for  $g(X_{LM}, \rho_T, T) = 0$ .

Therefore the chain rule only holds in the regions between the saturation boundaries and the critical isochore for both the liquid volume and liquid mass fractions in figs. 1 and 2 respectively. This may be a reason for the ambiguity of the limits for the derivatives when the critical point is approached from these regions. To avoid this ambiguity then, approach the critical point along  $\rho_c$  (figs. 1 and 2) or  $X_{c,LIM}$  (figs. 3 and 4).

Along  $\rho_c$ ,

$$\left. \frac{\partial X_{LV,c}}{\partial T} \right|_{\rho_T = \rho_c} = \frac{dX_{LV,c}}{dT} \equiv X'_{LV,c} \quad (81)$$

$$\left. \frac{\partial X_{LM,c}}{\partial T} \right|_{\rho_T = \rho_c} = \frac{dX_{LM,c}}{dT} \equiv X'_{LM,c} ,$$

independent of the derivatives and their limits found previously.

Figure 1 shows that  $X_{LV,c}$  has positive values virtually to the critical point. The argument that  $X_{LV,c}$  does not have a maximum (i.e.,  $X'_{LV,c} = 0$ ) except perhaps at  $T_c$  is as follows. There are only two possibilities for a maximum in  $X_{LV,c}$  in the interval  $T_{TP} < T < T_c$ . The first is illustrated graphically in fig. 8.

The locus of  $X_{LV,MAX}$  in fig. 8, stops at point "a" for some  $T < T_c$ . But it has been shown that eq. (18) describes, for all  $T < T_c$ ,  $X_{LV,MAX}$ . In addition, eq. (67) indicates that  $X_{LV,MAX} = X_{c,LIM}$  at  $T_c$ . Therefore this case could not exist, i.e., point "a" and  $X_{c,LIM}$  of fig. 8 must be the same point. This leads to the second possibility shown graphically in fig. 9.

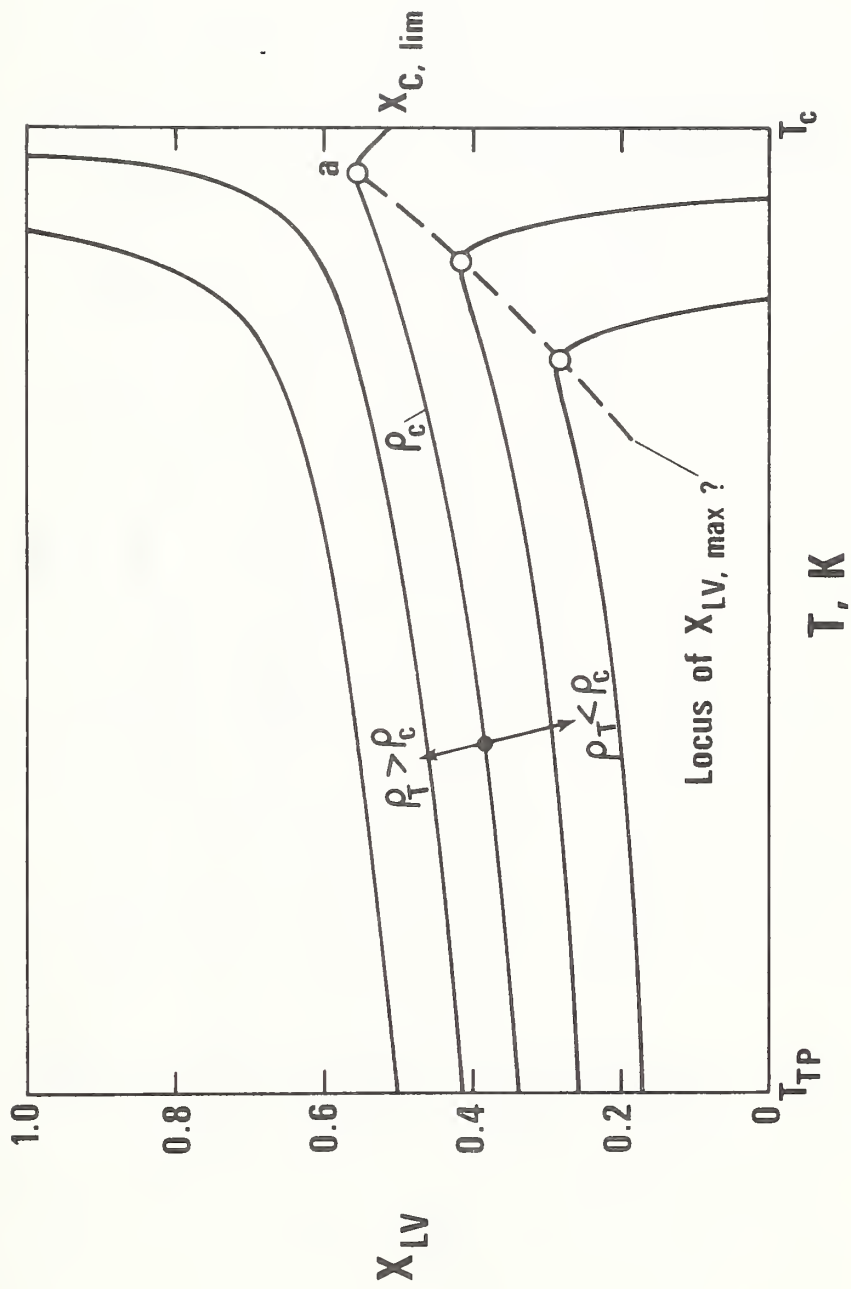


Figure 8.  $X_{LV, MAX}$  First Possibility.

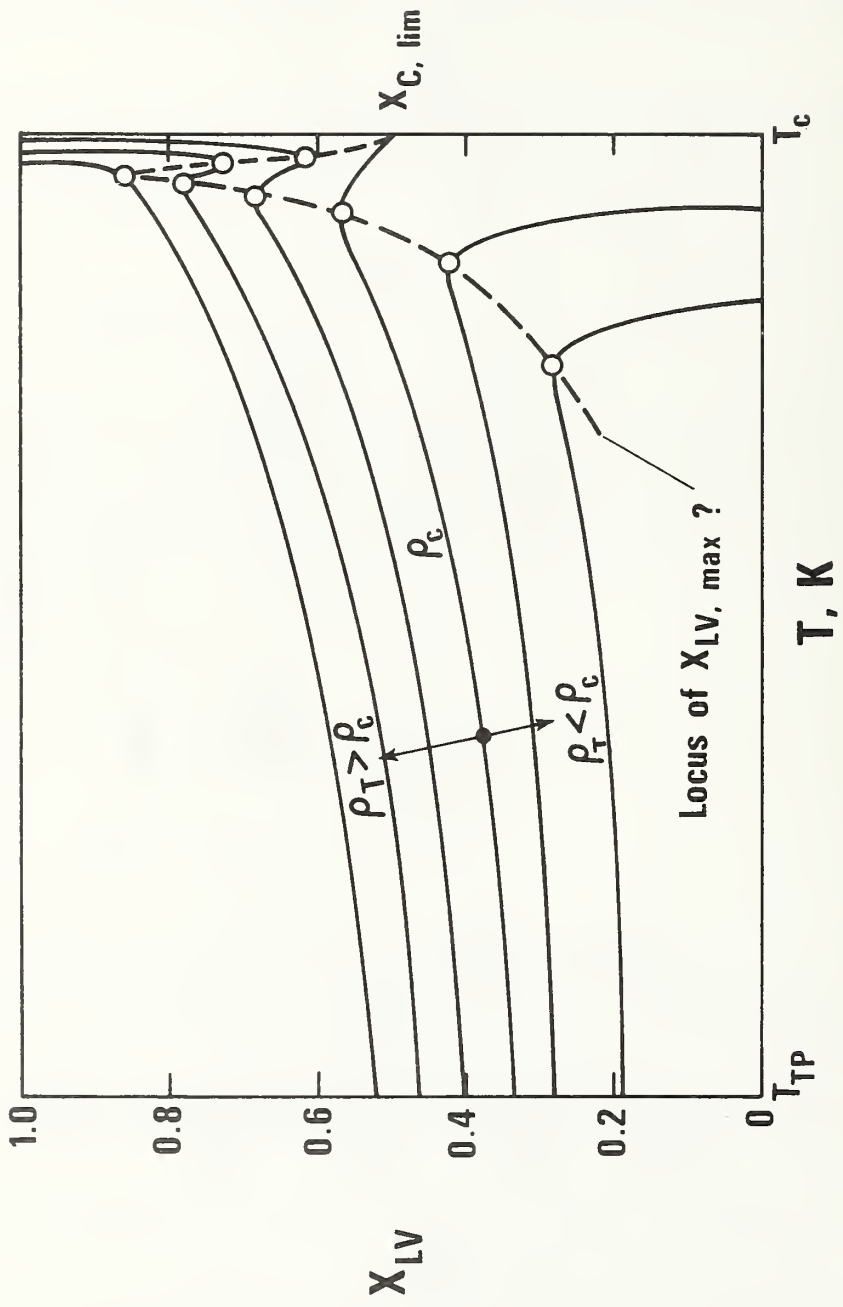


Figure 9.  $X_{LV, MAX}$  Second Possibility.

Here the locus of the zeros in  $X_{LV}$  is shown going into the critical point. However, for  $\rho_T > \rho_c$  a maximum and a minimum occurs in  $X_{LV}$ . Now at these "zero slope points" the value of  $\rho_T$  is given by eq. (19).

In order for the case of fig. 9 to exist, it would be necessary, at two different temperatures, for the right hand side of eq. (19) to be the same (for  $\rho_T > \rho_c$  in the example). This behavior in  $X_{LV}$  has never been found by this author even when working with data very near the critical point. An example of data close to the critical point is shown in fig. 10 based on oxygen data of Weber [7] in a one-half degree interval before the critical point. The departures from smooth curves can only be attributed to experimental error and certainly the points lie on the smooth curves "within" that error. The only data which might cause the reader to suspect the phenomena suggested in fig. 9 is that at 154.560 K in fig. 10 (second to the last temperature). But this "upward" trend appears at densities above and below the critical point and can most likely be attributed to an experimental bias. (The critical isochore appears to approach a value of  $X_{c,LIM}$  very near one-half.)

To further amplify the idea that the case of fig. 9 does not occur, data based on "dome" equations similar to eqs. (47) and (48) are presented. The equations are those of Douslin, et al. [8] for ethylene. They are:

$$\rho_L = 7.635 + 1.9695 \epsilon^{.350} + .02669 \epsilon^{.984} - .2731 \times 10^{-3} \epsilon^{1.618} \quad (82)$$

$$\rho_V = 7.635 - 1.9695 \epsilon^{.350} + .01404 \epsilon^{.984} + .6783 \times 10^{-3} \epsilon^{1.618} \quad (83)$$

These were substituted into eq. (24) for  $X_{LV,c}$  and eq. (18) for  $X_{LV,MAX}$ . The results are given in table 1.

Equations (82) and (83), based on theory and fit to actual data, result in an  $X_{LV,c}$  which has a positive slope and is monotonic to the critical point. Also  $X_{LV,MAX}$ , with a positive slope, increases monotonically into the critical point. The behavior shown in table 1 coincides with that of fig. 1 and also reinforces the result of the last section that  $\lim_{T \rightarrow T_c} X_{LV,MAX} = X_{c,LIM}$ .

The conclusion is that the cases shown in figs. 8 and 9 do not occur. Therefore  $X_{LV,c}$  does not have a zero slope except perhaps at the critical point. That is, the behavior of  $X_{LV,c}$  in fig. 8 is incorrect mathematically and there is no evidence for the behavior of  $X_{LV,c}$  as shown in fig. 9. The result is as suggested in fig. 1, that  $X_{LV,c}$  continues monotonically into  $X_{c,LIM}$  and, that the possibilities for  $X'_{LV,c}$  are:

$$0 \leq \lim_{T \rightarrow T_c} X'_{LV,c} \leq + \infty \quad (84)$$

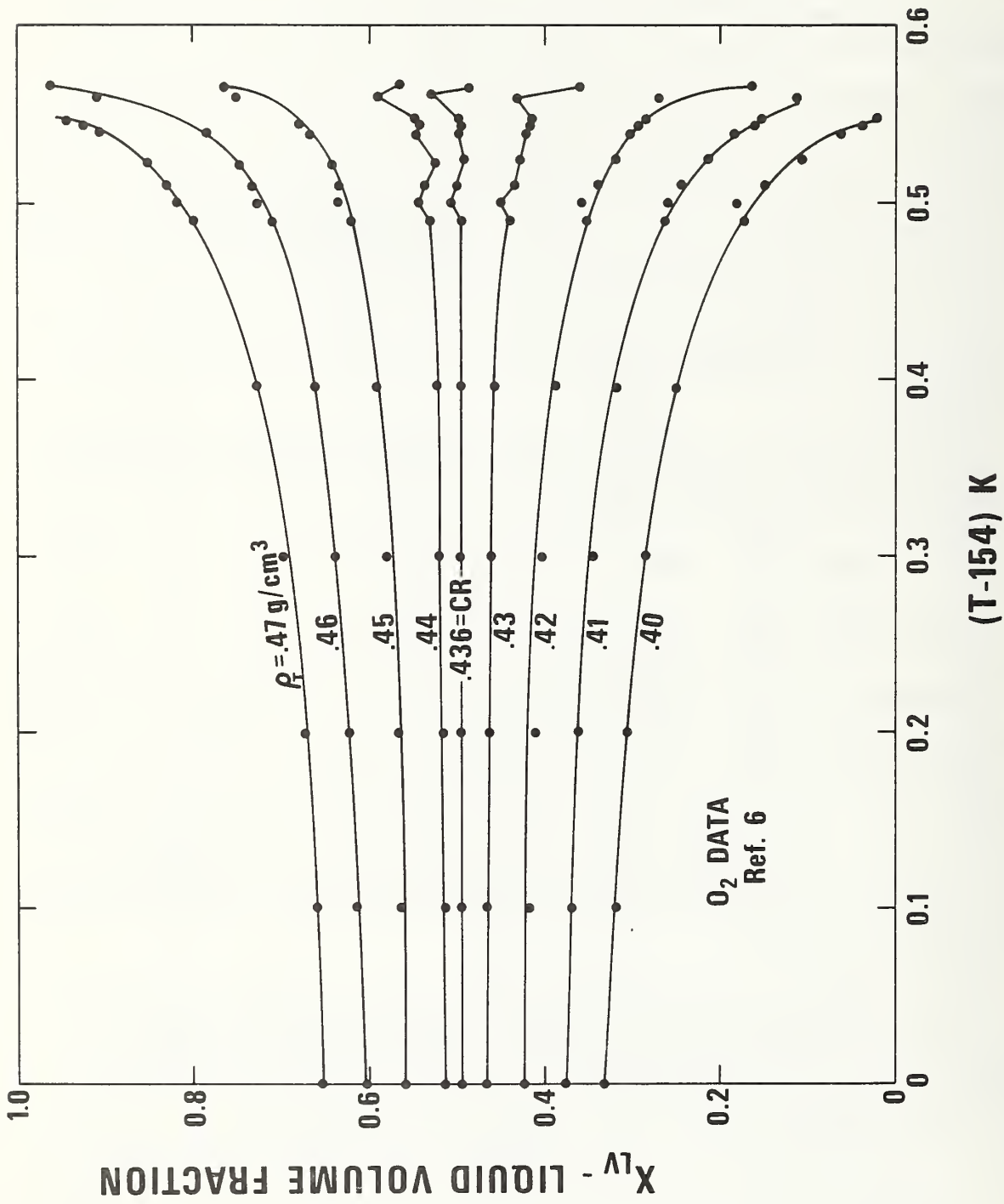


Figure 10. Data for  $X_{LV,MAX}$  Possibility Analysis.

Table 1.  $X_{LV,C}$  and  $X_{LV,MAX}$  for Ethylene

<u>T (K)</u>	<u><math>X_{LV,C}</math></u>	<u><math>X_{LV,MAX}</math></u>
0.1 K INTERVALS		
280.05	.4911	.4750
280.15	.4914	.4757
280.25	.4916	.4764
280.35	.4919	.4771
280.45	.4922	.4779
280.55	.4924	.4786
280.65	.4927	.4794
280.75	.4930	.4802
280.85	.4933	.4810
280.95	.4935	.4818
281.05	.4938	.4827
281.15	.4942	.4835
281.25	.4945	.4844
281.35	.4948	.4853
281.45	.4951	.4863
281.55	.4955	.4873
281.65	.4959	.4883
281.75	.4962	.4894
281.85	.4966	.4906
281.95	.4971	.4918
282.05	.4976	.4932
282.15	.4981	.4947
282.25	.4988	.4966
0.01 K INTERVALS		
282.26	.4989	.4968
282.27	.49896	.4971
282.28	.49904	.4973
282.29	.49913	.4975
282.30	.49923	.4978
282.31	.49933	.4981
282.32	.49944	.4984
282.33	.49957	.4988
282.34	.49972	.4992
282.35 ( $T_c$ )	.50000	.4999

Having established eq. (84), further analysis can be done by developing the derivative  $X'_{LV,c}$  in terms of eqs. (47) and (48). For convenience set  $\phi_l = \phi_v$ , an assumption usually made. (See eqs. (82) and (83) where Douslin, et al. [8] have  $\phi_l = \phi_v = .984$ .) The equation is as follows:

$$X'_{LV,c} = \frac{(B_{1l}B_{2v} - B_{2l}B_{1v})(\phi - \beta) \epsilon^{-\beta+\phi-1} + \text{TERMS}(\epsilon^{\text{EXP}>0})}{(B_{1l} - B_{1v})^2 + \text{TERMS}(\epsilon^{\text{EXP}>0})} , \quad (85)$$

and eq. (84) allows the limit of this derivative to be either zero, positive finite, or positive infinity.

Before the exponents are examined, the nature of the constant coefficient  $(B_{1l}B_{2v} - B_{2l}B_{1v})$  should be analyzed. The possibilities for it are either zero or greater than zero based on eq. (85). If it is to be zero then:

$$\frac{B_{1l}}{B_{1v}} = \frac{B_{2l}}{B_{2v}} \quad (86)$$

Since it has been previously shown that  $B_{1l}$  and  $B_{1v}$  have opposite algebraic signs, eq. (86) would mean that  $B_{2l}$  and  $B_{2v}$  would also have opposite signs. Sengers, et al. [4] in an extensive study of data near the critical point suggest that no conclusion can be made that  $B_{2l} = B_{2v}$  but indicate that when taking the difference  $\rho_l - \rho_v$  the  $B_{2l}$  and  $B_{2v}$  terms are nearly equal in magnitude and are of the same sign. The eqs. (82) and (83) of Douslin, et al., indicate that  $B_{2l} = .02669$  and  $B_{2v} = .01404$ , i.e., they are of the same sign.

It is reasonable then to suggest that since no evidence exists for assuming eq. (86),  $(B_{1l}B_{2v} - B_{2l}B_{1v}) > 0$  .

An examination of eq. (85) in the light of eq. (87) would result in the virtual elimination of zero as a limit for the derivative. Also, since the exponent  $(-\beta + \phi - 1)$  is not equal to zero itself the choice of the positive finite limit is also removed. The only reasonable choice left is that:

$$\lim_{T \rightarrow T_c} X'_{LV,c} = + \infty \quad (88)$$

The derivative  $X'_{LV,c}$  behaves as though the fluid were a "liquid" at the critical point (see fig. 1) and eq. (75).

A check of eqs. (82) and (83) for ethylene indicates that indeed eq. (87) is satisfied, i.e.,  $(1.9695)(.01404) - (-1.9695)(.02669) > 0$ , affirming that:

$$\lim_{T \rightarrow T_c} X'_{LV,c} = + \infty .$$

The data of table 1 indicates that the  $X_{LV,c}$  function comes into  $X_{c,LIM}$  with a very small slope and therefore must then turn upward virtually at  $T_c$ .

An exception to eq. (87) was found in the recent paper of Haar, et al. [9] for ammonia. His values are:

$$B_{1l} = 2.117$$

$$B_{1v} = -2.117$$

$$B_{2l} = -1.4097$$

$$B_{2v} = -1.1390$$

Indeed,  $B_{2l}$  and  $B_{2v}$  have the same sign but

$$(2.117)(-1.4097) - (-2.117)(-1.1390) < 0 ,$$

which would indicate  $\lim_{T \rightarrow T_c} X'_{LV,c} = -\infty$ . However the equations are based mainly

on data by Cragoe, et al [10,11] which are at best some 30 K away from the critical point. These equations were used only to estimate  $T_c$  and  $\rho_c$  and were not used in the determination of the published saturation data.

To check the ammonia data for the slope  $X'_{LV,c}$  at the critical point, this author fit the published saturation data from 116 - 132<sup>o</sup>C to the function  $X_{LV,c}$  ( $T_c = 132.24^o$ C). The procedure is outlined in a previous paper [6]. The results for an unweighted least squares fit is (Var (data) = .2547 x 10<sup>-7</sup>):

$$X_{LV,c} = (1/2) [1 - 3.903 \times 10^{-3} \epsilon^{.97}] \quad (89)$$

from which:

$$X'_{LV,c} = (1.893 \times 10^{-3}) \epsilon^{-.03} . \quad (90)$$

Clearly the limit is:  $+\infty$ , which agrees with eq. (88).

The equation for the derivative of the critical liquid mass fraction,  $X'_{LM,c}$ , is developed from eqs. (47) and (48) assuming  $\phi_v = \phi_l$ . The result is:

$$X'_{LM,c} = \frac{\left[ \left[ \beta(B_{1l}-B_{1v})(B_{1l}B_{1v}) \epsilon^{\beta-1} + \rho_c^2(\phi-\beta)[B_{1l}B_{2v}-B_{2l}B_{1v}] \epsilon^{\phi-\beta-1} \right. \right. \\ + \rho_c \left[ \{ 2\beta (B_{2l}-B_{2v}) + 2\phi B_{2l} \} B_{1l}B_{1v} \right. \\ + \phi \left. \left. \{ (B_{1l}-B_{1v}) B_{1l}B_{1v} - (B_{1v}+B_{1l}) B_{2l}B_{1v} \} \right] \epsilon^{\phi-1} \right. \\ \left. \left. + \text{TERMS } (\epsilon^{\text{EXP}>0}) \right] \right]}{\rho_c^2 (B_{1l} - B_{1v})^2 + \text{TERMS } (\epsilon^{\text{EXP}>0})} \quad (91)$$

The term containing  $\epsilon^{\beta-1}$  would have the strongest influence since

$$\begin{aligned}\beta-1 &\sim - .65 \\ \phi-\beta-1 &\sim - .35 \\ \phi-1 &\sim 0.0.\end{aligned}$$

The coefficient of  $\epsilon^{\beta-1}$ , i.e.,  $\beta(B_{1\ell}-B_{1V})(B_{1\ell}B_{1V})$  is  $< 0$  (assuming as before,  $B_{1\ell} > 0$  and  $B_{1V} < 0$ ). Hence the only choice for the limit of  $X'_{LM,c}$  is:

$$\lim_{T \rightarrow T_c} X'_{LM,c} = -\infty \quad (92)$$

This limit is also strongly suggested by the graph of fig. 2 for the critical isochore. The derivative  $X'_{LM,c}$  behaves as though the fluid were a "vapor" at critical point (see eq. (76)).

As previously stated, the liquid volume fraction derivative behaves as a "liquid" derivative, hence there is some ambiguity at the critical point in the derivatives in addition to the non-liquid, non-vapor ambiguous behavior of  $X_{LV,c}$  and  $X_{LM,c}$  themselves at the critical point.

From eq. (6):

$$X_{LV,c} = \frac{X_{LM,c} \rho_c}{\rho_\ell}.$$

The derivative with respect to temperature is

$$X'_{LV,c} = X'_{LM,c} \frac{\rho_c}{\rho_\ell} - \frac{X_{LM,c} \rho_\ell' \rho_c}{\rho_\ell^2}. \quad (93)$$

In the limit:

$$\lim_{T \rightarrow T_c} X'_{LV,c} = \lim_{T \rightarrow T_c} X'_{LM,c} - \frac{X_{c,LIM}}{\rho_c} \lim_{T \rightarrow T_c} \rho_\ell' \quad (94)$$

Since  $\rho_\ell'$  and  $X'_{LM,c}$  in the limit are  $-\infty$ ,

$$\lim_{T \rightarrow T_c} X'_{LV,c} = -\infty + \infty, \quad (95)$$

an indeterminate form. Thus the limit could be anything. The limit as given by eq. (75) ( $+\infty$ ) is allowed by eq. (95).

The ambiguity in the limit of the derivatives of eqs. (77), (78), (79) and (80), is avoided by accessing the critical point along the lines  $X_{LV} = X_{c,LIM}$  in fig. 3 and

$X_{LM} = X_{c,LIM}$  in fig. 4.

To that end, in eq. (11), substitute the derivatives from eqs. (47) and (48) and eq. (63) for  $X_{c,LIM}$  resulting in:

$$\left. \frac{\partial \rho_T}{\partial T} \right|_{X_{LV}=X_{C,LIM}} = \frac{\beta[B_{1l}B_{1v}-B_{1l}B_{1v}]e^{\beta-1} + \phi[B_{1v}B_{2l}-B_{1l}B_{2v}]e^{\phi-1} + \text{TERMS}(\epsilon^{\text{EXP}>0})}{(B_{1l} - B_{1v})} . \quad (96)$$

But the coefficient of  $\epsilon^{\beta-1}$  is zero hence:

$$\left. \frac{\partial \rho_T}{\partial T} \right|_{X_{LV}=X_{C,LIM}} = \frac{-\phi[B_{1l}B_{2v} - B_{1v}B_{2l}]e^{\phi-1} + \text{TERMS}(\epsilon^{\text{EXP}>0})}{(B_{1l} - B_{1v})} . \quad (97)$$

Earlier analysis indicates that it is reasonable to have  $(B_{1l}B_{2v} - B_{1v}B_{2l}) > 0$ , and since  $\phi$  and  $(B_{1l} - B_{1v})$  are greater than zero the possibilities are:

$$-\infty \leq \lim_{T \rightarrow T_c} \left. \frac{\partial \rho_T}{\partial T} \right|_{X_{LV}=X_{C,LIM}} \leq 0 \quad (98)$$

where the actual value is then determined by the value of  $\phi$ , i.e.,

$$0 < \phi < 1, \quad \lim_{T \rightarrow T_c} \left. \frac{\partial \rho_T}{\partial T} \right|_{X_{LV}=X_{C,LIM}} = -\infty, \quad (99)$$

$$\phi = 1, \quad \lim_{T \rightarrow T_c} \left. \frac{\partial \rho_T}{\partial T} \right|_{X_{LV}=X_{C,LIM}} = -\text{finite}, \text{ and} \quad (100)$$

$$\phi > 1, \quad \lim_{T \rightarrow T_c} \left. \frac{\partial \rho_T}{\partial T} \right|_{X_{LV}=X_{C,LIM}} = 0 . \quad (101)$$

There is much interest in the literature of today in the slope of the rectilinear diameter,  $(\rho'_l + \rho'_v)/2$ , especially at the critical point. Theoretical work by Green, et al. [3] and experimental work by Weiner, et al. [12] indicate the possibility of a slight "hook" in the rectilinear diameter, i.e., the hypothesis is that

$$\lim_{T \rightarrow T_c} \frac{(\rho'_v + \rho'_l)}{2} = -\infty \quad (102)$$

If in eq. (11),  $X_{LV} = 1/2$ , then:

$$\left. \frac{\partial \rho_T}{\partial T} \right|_{X_{LV}=1/2} = \frac{\rho'_V + \rho'_L}{2} \quad (103)$$

the slope of the rectilinear diameter.

The slope of the rectilinear diameter may be obtained by using the derivatives of eqs. (47) and (48) directly for  $\rho'_L$  and  $\rho'_V$  obtaining,

$$\rho'_L + \rho'_V = -\beta (B_{1L} + B_{1V}) \epsilon^{\beta-1} - \phi (B_{2L} + B_{2V}) \epsilon^{\phi-1} + \text{TERMS } (\epsilon^{\text{EXP} > 0}) \quad (104)$$

The variables of interest in eqs. (97), (103), and (104) are  $B_{1L}$ ,  $B_{1V}$ , and the exponent  $\phi$ . In eq. (104), it is assumed that if  $(B_{1L} + B_{1V}) \neq 0$  the  $\epsilon^{\beta-1}$  dominates. Table 2 summarizes the effect of varying  $B_{1L}$ ,  $B_{1V}$  ( $X_{C,LIM} = -B_{1V}/(B_{1L} - B_{1V})$ ) and  $\phi$ .

Table 2. Effect of  $\phi$ ,  $B_{1L}$ , and,  $B_{1V}$  on  $\lim_{T \rightarrow T_c} \left. \frac{\partial \rho_T}{\partial T} \right|_{X_{LV}=X_{C,LIM}}$  and  $\lim_{T \rightarrow T_c} (\rho'_L + \rho'_V)$

$X_{C,LIM}$	$\phi$	$\lim_{T \rightarrow T_c} \left. \frac{\partial \rho_T}{\partial T} \right _{X_{LV}=X_{C,LIM}}$	$\lim_{T \rightarrow T_c} (\rho'_L + \rho'_V)$
$(\frac{1}{2}, \left  B_{1V} \right  < \left  B_{1L} \right )$	<1	$-\infty$ (97) <sup>1</sup>	$-\infty$ (104)
	=1	-FINITE (97)	$-\infty$ (104)
	>1	0 (97)	$-\infty$ (104)
$(\frac{1}{2}, \left  B_{1V} \right  = \left  B_{1L} \right )$	<1	$-\infty$ (97)	$-\infty$ (97,103)
	=1	-FINITE (97)	-FINITE (97,103)
	>1	0 (97)	0 (97,103)
$(\frac{1}{2}, \left  B_{1V} \right  > \left  B_{1L} \right )$	<1	$-\infty$ (97)	$+\infty$ (104)
	=1	-FINITE (97)	$+\infty$ (104)
	>1	0 (97)	$+\infty$ (104)

<sup>1</sup>The number in parentheses refers to the related equation.

When  $B_{1L} = -B_{1V}$  ( $X_{C,LIM} = 1/2$ ), the rectilinear diameter slope is found

from eq. (97) as  $\left. \frac{\partial \rho_T}{\partial T} \right|_{X_{LV}=X_{C,LIM} = \frac{1}{2}}$  and  $\frac{\rho'_L + \rho'_V}{2}$  are equal (see eq. (103)). These should

match the values obtained from eq. (104) where at first order symmetry,  $B_{1L} = -B_{1V}$ , eq. (104) reduces to:

$$\rho'_l + \rho'_v = -\phi(B_{2l} + B_{2v}) \epsilon^{\phi-1} + \text{TERMS } (\epsilon^{\text{EXP}>0}) \quad (105)$$

From the values in table 2 for  $\lim (\rho'_l + \rho'_v)$ , at  $B_{1l} = -B_{1v}$  (based on eq. (97)) there are the following implications, given in table 3, for  $(B_{2l} + B_{2v})$  since, as said above, the values in eq. (105) should match.

Table 3. Analysis of  $(B_{2l} + B_{2v})$  for  $(B_{1l} = -B_{1v})$

$\phi$	$\lim_{T \rightarrow T_c} (\rho'_l + \rho'_v)$	$(B_{2l} + B_{2v})$
$< 1$	$-\infty$ (97) <sup>2</sup>	$> 0$ (105)
$= 1$	-FINITE (97)	$> 0$ (105)
$> 1$	$0$ (97)	NO RESTRICTION (105)

<sup>2</sup>The number in parentheses refers to the related equation.

If first order symmetry is assumed ( $B_{1l} = -B_{1v}$ ), and if  $\phi < 1$ , both generally assumed to be valid, then:

$$(B_{2l} + B_{2v}) > 0 \quad (106)$$

We see that for Douslin's [8] eqs., (82) and (83), both  $B_{2l}$  and  $B_{2v}$  are positive so the criterion is met. The  $B_{2l}$  and  $B_{2v}$  of Haar, et al. [9] for ammonia are both negative but see the previous discussion regarding the validity of these values in light of the data range from which they were derived.

Figure 11 indicates that if the rectilinear diameter is to have a slope in the limit of  $+\infty$ , the diameter must have the value of  $\rho_c$  two times, i.e., once at  $T_a$  (point "a") and again at the critical point. This author does not know of any evidence in the literature for such an occurrence. A reasonable hypothesis is then:

$$X_{c,LIM} \leq 1/2 \quad (107)$$

An expression for the derivative  $\left. \frac{\partial \rho_T}{\partial T} \right|_{X_{LM}}$  along  $X_{c,LIM}$  (see fig. 4) can also be developed. Utilizing eqs. (7), (16), (67), (68) and the derivatives of eqs. (47) and (48),

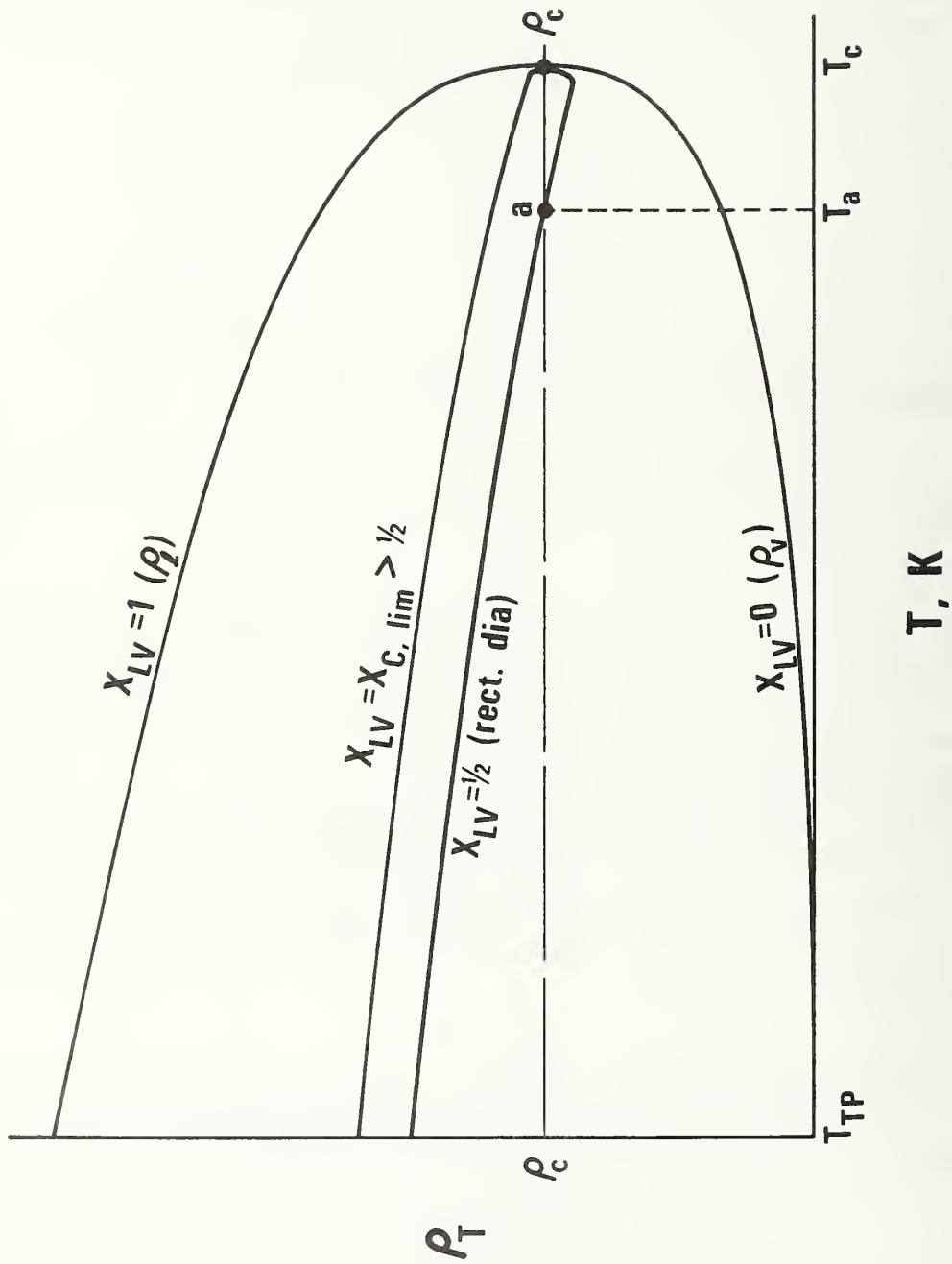


Figure 11. Implications of  $X_{C,LIM} > 1/2$ .

$$\frac{\partial \rho_T}{\partial T} \Big|_{X_{LM}=X_{c,LIM}} = \left[ \begin{aligned} & - (B_{1l} - B_{1v}) B_{1l} B_{1v} \beta \rho_c^2 \epsilon^{2\beta-1} \\ & - (B_{1l} B_{2v} - B_{1v} B_{2l}) \phi \rho_c^2 \epsilon^{\phi-1} \\ & + \text{TERMS } (\epsilon^{\text{EXP}>0}) \end{aligned} \right] \\ + \text{FINITE NO.} + \text{TERMS } (\epsilon^{\text{EXP}>0}) \quad (108)$$

Since,  $(B_{1l} - B_{1v}) > 0$ ,  $B_{1l} B_{1v} < 0$ , and the term  $\epsilon^{2\beta-1}$  dominates near the critical point,

$$\lim_{T \rightarrow T_c} \frac{\partial \rho_T}{\partial T} \Big|_{X_{LM}=X_{c,LIM}} = + \infty \quad (109)$$

regardless of what  $X_{c,LIM}$  is.

A brief analysis was made regarding insights into the rectilinear diameter in light of eq. (108). No additional information was found beyond that already reported.

The inequalities of eqs. (42) and (46) were investigated in the limit as  $T \rightarrow T_c$ . By use of the derivatives of eqs. (47) and (48) it can be shown that,

$$\lim_{T \rightarrow T_c} \left| \rho_v'' \rho_l' \right| = \lim_{T \rightarrow T_c} \left| \rho_l'' \rho_v' \right|. \quad (110)$$

Equations (82) and (83) for ethylene were used to demonstrate the validity of eq. (42) and eq. (110). The results are given in table 4.

A similar limit analysis for the inequality of eq. (46) was attempted with no conclusive result. However, the computer generated results of table 4 indicate that, not only is eq. (46) valid but also most likely,

$$\lim_{T \rightarrow T_c} \left| -\rho_v \rho_l \rho_l'' \rho_v' + 2\rho_v' \rho_l' (\rho_l' \rho_v - \rho_v' \rho_l) \right| = \lim_{T \rightarrow T_c} \left| \rho_v \rho_l \rho_v'' \rho_l' \right|. \quad (111)$$

Table 4. Check on Inequalities for Ethylene

T (K)	$ \rho'_L \rho''_V  >  \rho'_V \rho''_L $		$ \rho'_V \rho''_L \rho''_L \rho'_V + 2\rho'_V \rho'_L (\rho'_L \rho'_V - \rho'_V \rho'_L)  >  \rho'_V \rho''_L \rho''_V \rho'_L $	
	$\rho'_L \rho''_V$	$\rho'_V \rho''_L$	$-\rho'_V \rho''_L \rho''_L \rho'_V + 2\rho'_V \rho'_L (\rho'_L \rho'_V - \rho'_V \rho'_L)$	$\rho'_V \rho''_L \rho''_V \rho'_L$
242.15	-.970E-4	-.420E-4	.540E-2	-.192E-2
247.15	-.127E-3	-.604E-4	.794E-2	-.285E-2
252.15	-.173E-3	-.907E-4	.121E-1	-.440E-2
257.15	-.252E-3	-.145E-4	.193E-1	-.723E-2
262.15	-.402E-3	-.252E-3	.332E-1	-.130E-1
267.15	-.737E-3	-.507E-3	.650E-1	-.269E-1
272.15	-.175E-2	-.133E-2	.161	-.726E-1
277.15	-.777E-2	-.653E-2	.718	-.369
282.15	-.127E+2	-.124E+2	.942E+3	-.724E+3

(The following is for an increasingly finer  $\Delta T$ .)

282.25	-.622E+2	-.613E+2	.443E+4	-.358E+4
282.30	-.305E+3	-.303E+3	.210E+5	-.177E+5
282.33	-.250E+4	-.249E+4	.165E+6	-.145E+6
282.34	-.1232E+5	-.1228E+5	.794E+6	-.716E+6
and for $T_c$				
282.35	-.40274E+24	-.40274E+24	.23480E+26	-.23477E+26

### 3.4 Maxima and Minima Analysis as T Goes to $T_{TP}$

Figures 3 and 4 indicate that the following limits obtain at the triple point:

$$\lim_{\substack{T \rightarrow T_{TP} \\ X_{LV} \rightarrow 0^+}} \left. \frac{\partial \rho_T}{\partial T} \right|_{X_{LV}} = 0 \quad (112)$$

$$\lim_{\substack{T \rightarrow T_{TP} \\ X_{LV} \rightarrow 1^-}} \left. \frac{\partial \rho_T}{\partial T} \right|_{X_{LV}} = - \text{FINITE VALUE} \quad (113)$$

$$\lim_{\substack{T \rightarrow T_{TP} \\ X_{LM} \rightarrow 0^+}} \left. \frac{\partial \rho_T}{\partial T} \right|_{X_{LM}} \cong 0 \quad \text{or} \quad + \text{FINITE} \quad (114)$$

$$\lim_{\substack{T \rightarrow T_{TP} \\ X_{LM} \rightarrow 1^-}} \left. \frac{\partial \rho_T}{\partial T} \right|_{X_{LM}} = 0 \quad . \quad (115)$$

Hypothesize that eqs. (32) and (112) simultaneously hold at the triple point. Equation (112) implies that  $X_{LV,MAX} \rightarrow 0$  and  $\rho_{T,MAX} \rightarrow \rho_{V,TP}$  as  $T \rightarrow T_{TP}$ . The corresponding  $X_{LM,MAX}$  at  $\rho_{T,MAX} = \rho_{V,TP}$  is:

$$X_{LM,MAX} = \frac{\rho_{L,TP}}{\rho_{V,TP}} \left[ \frac{\rho_{V,TP} - \rho_{V,TP}}{\rho_{L,TP} - \rho_{V,TP}} \right] = 0 \quad .$$

But eq. (32) says that  $X_{LM,MAX} > X_{LV,c}$  and  $X_{LV,c}$  is usually about .3 or .4 at the triple point (see fig. 1) so our original hypothesis is wrong.

Hypothesize that eqs. (32) and (115) simultaneously hold at the triple point. Equation (115) implies that  $X_{LM,MIN} \rightarrow 1$  and  $\rho_{T,MIN} \rightarrow \rho_{L,TP}$ . The corresponding  $X_{LV,MIN}$  at  $\rho_{T,MIN} = \rho_{L,TP}$  is:

$$X_{LV,MIN} = \frac{\rho_{L,TP} - \rho_{V,TP}}{\rho_{L,TP} - \rho_{V,TP}} = 1$$

But eq. (32) says that  $X_{LM,c} > X_{LV,MIN}$ . While  $X_{LM,c}$  is very close to one, about .998, or so, at the triple point it can never be one because  $\rho_c \neq \rho_{L,TP}$  (also see fig. 1). So this hypothesis is also wrong. The conclusion is that eq. (32) does not hold at the triple point.

Equations (112) and (114) would appear to be expressions for  $\rho_v'$  at the triple point and eqs. (113) and (115) appear to be values of  $\rho_l'$  at the triple point. However, the ambiguity is obvious. Again, as at the critical point, this ambiguity of definition of the derivative may be due to the inapplicability of eqs. (8) and (13) along the saturation lines as has been already mentioned. Thus, the only non-ambiguous limit for  $\rho_v'$  and  $\rho_l'$  at the triple point can be found along the saturated vapor and saturated liquid lines respectively as  $T \rightarrow T_{TP}$ .

In the light of the behavior of the liquid volume and liquid mass fractions, the triple point exhibits singularities of the same sort as the critical point particularly as to ambiguity in the derivatives.

#### 4. CORRELATING COEXISTENCE - CRITICAL POINT DATA USING THE LIQUID VOLUME FRACTION

An earlier paper by this author [6] outlined a method of testing whether or not the saturation density data correlated with published critical point data. The technique is based on fig. 1 and its subsequent analysis. If, as the critical liquid volume fraction

approached  $T_c$ , it went through a maximum, the  $\rho_c$  used was too low, i.e., in reality it was a  $\rho_v$ . Or, if, as the critical liquid volume fraction approached  $T_c$ , it increased beyond one-half and kept increasing, the  $\rho_c$  used was too high, i.e., in reality it was a  $\rho_l$ .

In that earlier paper it was assumed that the critical liquid volume fraction is one-half at the critical point. This assumption was based on the work by Sengers, et al. [4]. The macroscopic approaches of this current paper, could only indicate that the fraction concerned is equal to or less than one-half at the critical point. The value one-half is, however, assumed for the work that follows. The one-half is a reasonable answer to the ambiguity at the critical, i.e., the fraction is not zero (a vapor) or one (a liquid). A further aspect of the value one-half is that it implies a first order symmetry ( $B_{1l} = -B_{1v}$ ) at the critical point, i.e., from eq. (63):

$$X_{C,LIM} = -B_{1v}/(B_{1l} - B_{1v}) = 1/2 \text{ for } (B_{1l} = -B_{1v}) \quad (116)$$

A look at the ratio of the derivatives  $\rho'_l$  and  $\rho'_v$  further emphasizes the nature of first order symmetry. From eqs. (47) and (48) and ( $\beta_l = \beta_v = \beta$ ) the following ratio may be calculated:

$$\frac{\rho'_l}{\rho'_v} = \frac{-B_{1l}\beta\epsilon^{\beta-1} - B_{2l}\phi_l\epsilon^{\phi_l-1} - B_{3l}\psi_l\epsilon^{\psi_l-1}}{-B_{1v}\beta\epsilon^{\beta-1} - B_{2v}\phi_v\epsilon^{\phi_v-1} - B_{3v}\psi_v\epsilon^{\psi_v-1}} \quad (117)$$

Dividing by  $\epsilon^{\beta-1}$ , taking the  $\lim T \rightarrow T_c$  ( $\epsilon \rightarrow 0$ ), the result is

$$\lim_{T \rightarrow T_c} \frac{\rho'_l}{\rho'_v} = \frac{B_{1l}}{B_{1v}} \quad , \quad (118)$$

and if ( $B_{1l} = -B_{1v}$ ) (first order symmetry),

$$\lim_{T \rightarrow T_c} \frac{\rho'_l}{\rho'_v} = -1 \quad . \quad (119)$$

This ratio of minus one also agrees with the idea that at the critical point neither the liquid or vapor is dominant thus carrying out the theme of ambiguity at the critical point. As a further indication that  $X_{C,LIM}$  is one-half, the reader may refer to fig. 1 for methane and fig. 10 for oxygen. In both cases the graph indicates that the critical isochore on a  $X_{LV}$  vs  $T$  plot comes to nearly one-half at the critical point. It is assumed, in the analysis that follows, that  $X_{C,LIM}$  is one-half.

The behaviorial test for  $X_{LV}$  is applied below to argon data published by Gosman, et al. [13]. The results are shown in table 5.

Table 5.  $X_{LV,c}$  vs T for Argon

( $\rho_c = 13.4123$  mol/L pub)

<u>T (K)</u>	<u><math>X_{LV,c}</math></u>
145.00	.4762
146.00	.4777
147.00	.4790
148.00	.4795
149.00	.4781
150.00	.4693
150.860 ( $T_c$ )	(.5000)

The published  $\rho_c$  (13.4123 mol/L) is behaving more like a  $\rho_v$  since the  $X_{LV,c}$  function turns down before  $T_c$  is reached. These same six data points were fit to a functional form of  $X_{LV,c}$  by this author. From this fit an estimate of  $\rho_c$  can be made. (The details of this procedure are outlined later.)

The result from the unweighted least squares fit at a minimum variance of the data is:

$$\rho_c = 13.6138 \text{ mol/L}$$

$$\sigma_{\rho_c} = 0.0031$$

for an  $X_{c,LIM}$  assumed to be one-half.

This "correctly correlated"  $\rho_c$  is indeed higher than the published value as the "X" analysis predicts.

A similar analysis was done on more recent data - that of ammonia by Haar, et al. [9]. The results are shown in table 6. The second column of table 6 indicates that the proposed  $X_{LV,c}$  goes through a maximum and decreases towards zero. These data

(116 - 132°C) were then fit to an  $X_{LV,c}$  function with one-half at the critical point (Haar's assumption). The result is:

Table 6.  $X_{LV,c}$  vs T for Ammonia

T (°C)	$X_{LV,c}$ ( $\rho_c = .23502 \text{ g/cm}^3$ pub)	$X_{LV,c}$ ( $\rho_c = .23652 \text{ g/cm}^3$ from fit)
116	.4664	.4711
117	.4678	.4727
118	.4693	.4743
119	.4708	.4759
120	.4724	.4776
121	.4739	.4793
122	.4755	.4811
123	.4771	.4829
124	.4788	.4848
125	.4804	.4867
126	.4821	.4887
128	.4852	.4927
130	.4873	.4963
132	.4854	.4983
132.24 ( $T_c$ )	(.5000) ?	.5000

$$\rho_c = .23652 \text{ g/cm}^3$$

$$\sigma_{\rho_c} = .00004$$

Again the properly correlated  $\rho_c$  is slightly higher than the published value as the analysis would indicate. The results for  $X_{LV,c}$  using this new  $\rho_c$  are given in column three of table 6. The values go monotonically towards .5000 which is expected by the earlier analysis in this report. (This type of analysis had been done previously by this author [6] for data published by ASHRAE-American Society of Heating, Refrigeration, and Air Conditioning Engineers, Inc., 1969.)

The foregoing procedure for testing the correlation of saturation/critical data may be useful to those whose task it is to evaluate thermodynamic property data.

Ethylene data are also analyzed. Whereas, for the argon and ammonia, smoothed published data were used, the weighted experimental values of Douslin, et al. [8] are used for ethylene. The intent of the following is to present a method for obtaining a correctly correlated value for  $\rho_c$  directly from data. Arguments are presented to indicate the statistical soundness of the approach.

An outline of the procedure (reported in a previous paper [6]), used to fit  $X_{LV,c}$  to the data follows.

Substituting eqs. (47) and (48) into eq. (24) for the critical liquid volume fraction, results in a series of terms of  $\epsilon$  having exponents (not necessarily integers). For convenience, a truncated form of this series of terms for  $X_{LV,c}$  is assumed as follows:

$$X_{LV,c} = (X_{C,LIM})[1 + b(\epsilon)^P + c(\epsilon)^R] \quad (120)$$

where:

b,c are constants,

P,R are exponents (not necessarily integers),

$$\epsilon = T - T_c$$

and:

$$X_{LV,c} \rightarrow X_{C,LIM} \text{ as } \epsilon \rightarrow 0.$$

Combining eqs. (24) and (120) and doing some algebraic manipulation the result (with  $X_{C,LIM} = \text{one-half}$ ) is:

$$\rho_v + \rho_\ell = A + B(\epsilon)^P(\rho_\ell - \rho_v) + C(\epsilon)^R(\rho_\ell - \rho_v) \quad (121)$$

where:

$$A = 2\rho_c, B, C \text{ are constants.}$$

The exponents P and R are varied until the variance of the data for a least squares fit is minimized. The digital computer utilizes a Gauss Jordan pivoting technique yielding, among other things, the best estimate of  $\rho_c$  (A/2) and its standard deviation.

Whereas eq. (121) looks like the rectilinear diameter, it really is quite different as far as the data used in the fit is concerned. A normal fit of the rectilinear diameter uses only values of  $(\rho_\ell + \rho_v)/2$  while eq. (121) also utilizes the difference  $(\rho_\ell - \rho_v)$  which is inherently quite accurate (see Weber [7] for this opinion). Also eq. (121) is not an extrapolation to the critical point but (from eq. (120)) is a fit constrained to a particular value,  $X_{C,LIM} = \text{one-half}$ , at the critical point.

Equation (120) was fit (via eq. (121)) to the fourteen weighted data points presented by Douslin, et al. [8] for ethylene from 238.15 to 282.15 K ( $T_c = 282.35$  K). The data used are given in table 7 below. In fitting the data, first one exponential term in eq. (121) is utilized, and a minimum variation in the data is found. Then a second term is added in eq. (121) until a lower minimum in the variation of the data is found. Then the "local" area of these exponents is searched by successive approximations to check on a further minimization of the variance. A more sophisticated approach could be utilized in which the computer finds the "best fit" of exponents using a non-linear fit procedure. However, the  $\rho_c$  found is certainly correct in the first four significant figures - well within experimental accuracy. The results given in table 8, later presented, attest to the "goodness" of fit.

The use of only one term resulted in a systematic rather than a random error distribution found when using two exponential terms. The result of the weighted least squares fit is (for  $X_{C,LIM} = \text{one-half}$  which Douslin assumes):

$$\rho_l + \rho_v = 15.258577 + .011666548 \epsilon^{.528} (\rho_l - \rho_v) + .65778747 \times 10^{-3} \epsilon^{1.088} (\rho_l - \rho_v) \quad (122)$$

or in  $X_{LV,c}$  form:

$$X_{LV,c} = (.5)[1 - .011666548 \epsilon^{.528} - .65778747 \times 10^{-3} \epsilon^{1.088}] \quad (123)$$

and with a  $\rho_c$  found to be:

$$\rho_c = 7.6292884 \text{ mol/dm}^3$$

$$\sigma_{\rho_c} = 0.0000270 \text{ mol/dm}^3$$

Table 7. Experimental Ethylene Data  
(from Douslin, et al. [8])

T (K)	$\rho_l \left( \frac{\text{mol}}{\text{dm}^3} \right)$	$\rho_v \left( \frac{\text{mol}}{\text{dm}^3} \right)$	Weight
238.15	16.036	1.1130	1280
243.15	15.634	1.2986	1280
248.15	15.196	1.5141	1280
253.15	14.723	1.7672	1280
258.15	14.207	2.0677	1280
263.15	13.630	2.4321	1280
268.15	12.966	2.8905	1279
273.15	12.146	3.5025	1053
278.15	10.995	4.4471	775
279.15	10.674	4.7246	725
280.15	10.290	5.071	485
281.15	9.767	5.546	232
281.65	9.387	5.911	128
282.15	8.780	6.489	33
282.35 ( $T_c$ )	7.635	7.635	

<sup>3</sup>This  $\rho_c$  is from a straight line extrapolation of the rectilinear diameter.

If the derivative of eq. (123) is taken as  $T \rightarrow T_c$ , a limit of  $+\infty$  is obtained. This is in accordance with previous findings (see eq. (88)). Further, in reference to eq. (122), if, from scaling laws:

$$\rho_l - \rho_v \sim \epsilon^\beta, \quad (124)$$

the derivative  $(\rho'_l + \rho'_v)$  goes to  $-\infty$  which is predicted for  $\phi < 1$  ( $.350 + .528 = .878 < 1$ ) and  $X_{C,LIM} = \text{one-half}$ . This is in accordance with the results previously predicted and listed in table 2.

The critical temperature utilized is Douslin's value of 282.35 K. The  $\rho_c$  value calculated comes out slightly less than the value ( $7.635 \text{ mol/dm}^3$ ) presented by Douslin. An analysis of  $X_{LV,C}$  versus T using this value of 7.635, resulted in an  $X_{LV,C} = .5002$  at  $282.15 \text{ K} < T_c$ . This indicates that a correlated value for  $\rho_c$  must be slightly lower.

The fit of eqs. (122) and (123) to the data is shown in table 8. The percent differences are very small and indicate a random error which is statistically desirable. The results of the weighted least squares fit for ethylene are given below. For,

$$\rho_v + \rho_l = A + B(\epsilon)^P (\rho_l - \rho_v) + C(\epsilon)^R (\rho_l - \rho_v) \quad , \quad (121)$$

Table 8.  $X_{LV,C}$  and  $(\rho_l + \rho_v)$  Comparison for Ethylene

T (K)	$(\rho_l + \rho_v)^4$ , DATA	$(\rho_l + \rho_v)$ , CALC	% Diff	$X_{LV,C}$ , DATA	$X_{LV,C}$ , CALC	% Diff
				( $\rho_c = 7.6292884$ )		
238.15	17.149000	17.151151	-.0125	.43666075	.43658868	+.0165
243.15	16.932600	16.929469	+.0185	.44161226	.44172145	-.0247
248.15	16.710100	16.709095	+.0060	.44695462	.44699133	-.0082
253.15	16.490200	16.491149	-.0058	.45246827	.45243163	+.0081
258.15	16.274700	16.276070	-.0084	.45814737	.45809092	+.0123
263.15	16.062100	16.063816	-.0107	.46412170	.46404508	+.0165
268.15	15.856500	15.854547	+.0123	.47032786	.47042478	-.0206
273.15	15.648500	15.647636	+.0055	.47744414	.47749413	-.0105
278.15	15.442100	15.442076	+.0002	.48598610	.48598790	-.0004
279.15	15.398600	15.400722	-.0138	.48823216	.48805379	+.0365
280.15	15.361000	15.358999	+.0130	.49018747	.49037917	-.0391
281.15	15.313000	15.316183	-.0208	.49355328	.49317621	+.0764
281.65	15.298000	15.293720	+.0280	.49432923	.49494492	-.1246
282.15	15.269000	15.270265	-.0083	.49772519	.49744914	+.0555

<sup>4</sup>Density units is  $\text{mol/dm}^3$ .

$$A = .15258577 \times 10^{+2} = 2\rho_c; \text{Var}(A) = .29216971 \times 10^{-8}$$

$$B = .11666548 \times 10^{-1}; \text{Var}(B) = .82952522 \times 10^{-11}$$

$$C = .65778747 \times 10^{-3}; \text{Var}(C) = .10371048 \times 10^{-12}$$

$$\text{Cov}(A,B) = - .13428749 \times 10^{-9}$$

$$\text{Cov}(A,C) = + .13600825 \times 10^{-10}$$

$$\text{Cov}(B,C) = - .91386470 \times 10^{-12}$$

$$\text{Correlation Coefficient}(A,B) = - .86258752$$

$$\text{Correlation Coefficient}(A,C) = .78133331$$

$$\text{Correlation Coefficient}(B,C) = - .98527119$$

An analysis of each coefficient with its variance indicates that the value zero does not lie within a  $3\sigma$  confidence limit; hence, each coefficient is statistically significant. It is also desirable that the value ( $A = 2\rho_c$ ) be quite insensitive to the values of the coefficients B and C. Indeed, the correlation coefficients indicate that A does not correlate highly (statistically speaking) with B or C. The coefficients B and C are more highly correlated with each other. This is to be expected since they are each involved in similar type terms in eq. (121).

Another consideration is the sensitivity of  $\rho_c$  to changes in the exponents P and R. To analyze this, each exponent was held at its value found for the best fit while the other was varied until  $\rho_c$  could no longer be reproduced as  $7.629 \text{ mol/dm}^3$  within four significant figures. The results are shown below:

$$P = .528 \left\{ \begin{array}{l} R = 1.079, \quad \rho_c = 7.62947 \text{ (mol/dm}^3\text{)} \\ R = 1.088, \quad \rho_c = 7.62929 \quad \text{(Best Fit)} \\ R = 1.126, \quad \rho_c = 7.6285 \end{array} \right.$$

$$R = 1.088 \left\{ \begin{array}{l} P = .5306, \quad \rho_c = 7.62949 \\ P = .528, \quad \rho_c = 7.62929 \quad \text{(Best Fit)} \\ P = .5184, \quad \rho_c = 7.6285 \end{array} \right.$$

The results indicate that  $\rho_c$  is relatively insensitive to the exponents P and R, i.e., the critical density is not highly dependent on the functional form - a desirable result.

The fit, if statistically sound, should result in a randomly distributed error or percent error. Data given in table 8 indicate a random error. Also, fig. 12 gives error data in a deviation plot for eq. (122). The figure indicates a relatively random error.

Also, the question arises concerning the sensitivity of the critical density to changes in the critical temperature. Moldover [5] and Sengers [14] report values of  $T_c$

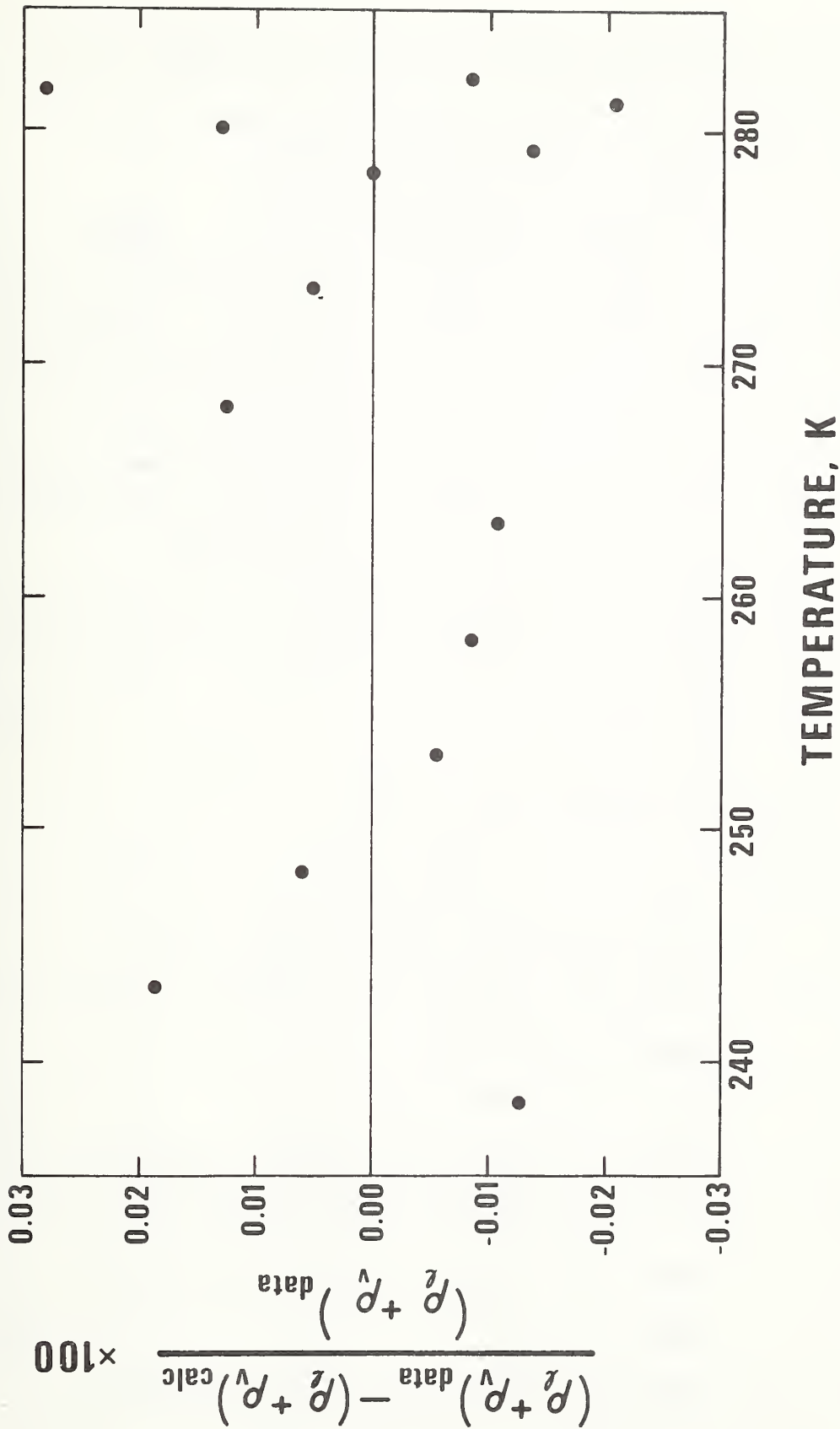


Figure 12. Percent Deviation Plot of  $\rho_l + \rho_v$  for Ethylene.

for ethylene differing slightly from Douslin's value of 282.35 K. Each of these temperatures was utilized in the  $X_{LV,c}$  fit with no change in the critical density to four significant figures. These results are summarized in table 9 below.

Table 9. Critical Properties of Ethylene

Source	$T_c$ (K)	$\rho_c$ (mol/dm <sup>3</sup> )	Method
Moldover [5]	282.344	7.650	Visual observation of critical
Douslin, et al. [8]	282.350	7.635	Graphical - $T_c$ ; Straight line extrapolation of rectilinear diameter - $\rho_c$
Sengers [14]	282.3452	7.634	Fit of single phase data to scaled equation of state
This report	Any of above	7.629	Fit of $X_{LV,c}$ vs $T$ to Douslin's saturation data

Having found  $\rho_c$  from the data and  $X_{LV,c}$  correlation it is possible to obtain an equation for  $\rho_\ell$  of the form:

$$\rho_\ell = \rho_c + B_{1\ell} \epsilon^\beta + B_{2\ell} \epsilon^\phi + B_{3\ell} \epsilon^\psi \quad (47)$$

where, following Douslin, et al. [8]:

$$\beta = .350 \quad (\text{found from a graph of } (\rho_\ell - \rho_v) \text{ vs } \epsilon)$$

$$\phi = \beta + 1/\epsilon \quad ,$$

$$\psi = \beta + 2/\epsilon \quad .$$

The equation resulting from a weighted least squares fit for  $\rho_\ell - \rho_c$  is:

$$\rho_\ell = 7.6292884 + 1.9752911 \epsilon^{.350} + .025699752 \epsilon^{.986} - .23107950 \times 10^{-3} \epsilon^{1.622} \quad (125)$$

compared to Douslin's equation repeated below.

$$\rho_\ell = 7.635 + 1.9695 \epsilon^{.350} + .02669 \epsilon^{.984} - .2731 \times 10^{-3} \epsilon^{1.618} \quad (82)$$

The fit of eq. (125) compared to eq. (82) is slightly better for one-half of the fourteen data points and slightly worse for the other half. The results are shown in table 10.

The next problem is to obtain values of  $\rho_v$ . Two approaches were utilized. The first approach was to combine eqs. (123) for  $X_{LV,c}$  and (125) for  $\rho_\ell$  and solve for  $\rho_v$ , i.e.,

$$\rho_{v,CALC} = (\rho_c - X_{LV,c} \rho_\ell) / (1 - X_{LV,c}) \quad (126)$$

The results for this calculation are shown in table 11. The overall fit is slightly better than that for Douslin's fit given in eq. (83).

Table 10.  $\rho_l$  (mol/dm<sup>3</sup>) Comparisons for Ethylene

T (K)	$\rho_{l,DATA}$	$\rho_{l,CALC}$ Equation (125)	$\rho_{l,DATA}-\rho_{l,CALC}$	% Diff	$\rho_{l,DATA}-\rho_{l,CALC}$ Equation (82)
238.15	16.036	16.037977	-.00198	-.0123	-.001
243.15	15.634	15.630700	+.00330	+.0211	+.003
248.15	15.196	15.195190	+.00081	+.0053	+.001
253.15	14.723	14.724569	-.00157	-.0107	-.002
258.15	14.207	14.208639	-.00164	-.0115	-.002
263.15	13.630	13.631159	-.00116	-.0085	-.001
268.15	12.966	12.963389	+.00261	+.0201	+.003
273.15	12.146	12.144977	+.00102	+.0084	+.001
278.15	10.995	10.996848	-.00185	-.0168	-.001
279.15	10.674	10.676468	-.00247	-.0231	-.002
280.15	10.290	10.287406	+.00259	+.0252	+.003
281.15	9.767	9.7651870	+.00181	+.0185	+.001
281.65	9.387	9.3907125	-.00371	-.0395	-.005
282.15	8.780	8.7591117	+.02088	+.2378	+.018

Table 11.  $\rho_v$  (mol/dm<sup>3</sup>) Comparisons for Ethylene

T (K)	$\rho_{v,DATA}$	$\rho_{v,CALC}$ Equation (126)	$\rho_{v,DATA}-\rho_{v,CALC}$	% Diff	$\rho_{v,DATA}-\rho_{v,CALC}$ Equation (83)
238.15	1.1130	1.1133772	-.000377	-.0339	-.0001
243.15	1.2986	1.2984076	+.000192	+.0148	+.0003
248.15	1.5141	1.5138464	+.000254	+.0168	+.0002
253.15	1.7672	1.7667706	+.000429	+.0243	+.0002
258.15	2.0677	2.0675788	+.000121	+.0059	-.0002
263.15	2.4321	2.4326972	-.000597	-.0245	-.0008
268.15	2.8905	2.8909751	-.000475	-.0164	-.0003
273.15	3.5025	3.5026075	-.000107	-.0031	+.0006
278.15	4.4471	4.4453302	+.001769	+.0398	+.0020
279.15	4.7246	4.7243203	+.000280	+.0059	+.0001
280.15	5.0710	5.0715327	-.000533	-.0105	-.0020
281.15	5.5460	5.5509046	-.004905	-.0884	-.0070
281.65	5.9110	5.9031244	+.007876	+.1332	+.0040
282.15	6.4890	6.5109346	-.021935	-.3380	-.0280

The other approach is to utilize the  $\rho_c$  found from  $X_{LV,c}$ , assume first order symmetry, and assume the exponents in the equation are the same as for  $\rho_\ell$  in eq. (125), and fit:

$$\rho_v - 7.6292884 + 1.9752911 \epsilon^{.350} = B_{2v} \epsilon^{.986} + B_{3v} \epsilon^{1.622} \quad (127)$$

The results are not as good as those obtained using eq. (126). The differences between  $\rho_{v,DATA}$  and  $\rho_{v,CALC}$  are about one order of magnitude higher than those in table 11. This is not satisfactory. The equation obtained was:

$$\begin{aligned} \rho_v = & 7.6292884 - 1.9752911 \epsilon^{.350} + .16287155 \times 10^{-1} \epsilon^{.986} \\ & + .50890319 \times 10^{-3} \epsilon^{1.622} \end{aligned} \quad (128)$$

Equations (125) for  $\rho_\ell$  and (128) for  $\rho_v$  meet the criteria of eqs. (87) and (106).

The following procedure is suggested for obtaining the critical temperature, density, and smooth saturation density values from experimental saturation data.

Step One: Plot  $\rho_\ell - \rho_v$  vs  $\epsilon$  on log-log paper to obtain a value for  $\beta$ . Use in addition, a computer analysis of this plot to obtain a best value of  $T_c$ . For this procedure see Weber [7]. This utilizes the well known scaling law:

$$\rho_\ell - \rho_v \sim \epsilon^\beta \quad (124)$$

Step Two: Utilize this  $T_c$  in a fit of the data to  $X_{LV,c}$  finding the best value of  $\rho_c$ .

Step Three: Utilize the  $\rho_c$ ,  $T_c$ , and  $\beta$  to fit the  $\rho_\ell$  data to an equation.

Step Four: Utilize the  $X_{LV,c}$  and  $\rho_\ell$  equations to generate smooth data for the saturation densities both  $\rho_\ell$  and  $\rho_v$ .

This procedure allows a rational integration of the critical and saturation properties. The  $X_{LV,c}$  function is the integration tool.

One of the major problems left in coexistence data work is to obtain equations which will fit the entire range from the triple to the critical point. The "dome" equations which are used here are not thought to be valid over this entire range. However, the relative flatness of the  $X_{LV,c}$  curves over this entire temperature range (see fig. 1) may be helpful in solving this problem.

Now,  $\rho_\ell$  from eq. (125) and  $\rho_v$  from eq. (126) can be utilized in a final statistical analysis of the original fit of eq. (121). This test is to look at the shape and magnitude of the  $3\sigma$  confidence band over the temperature range of interest. The standard deviation with temperature of the fit can be found from the square root of the variation of  $(\rho_\ell + \rho_v)$ . This variance, from well known statistical considerations, is:

$$\begin{aligned}
\text{Var}(\rho_\ell + \rho_v) = & \frac{\partial(\rho_\ell + \rho_v)}{\partial A} \left[ \frac{\partial(\rho_\ell + \rho_v)}{\partial A} \text{Var}(A) + \frac{\partial(\rho_\ell + \rho_v)}{\partial B} \text{Cov}(A,B) + \frac{\partial(\rho_\ell + \rho_v)}{\partial C} \text{Cov}(A,C) \right] \\
& + \frac{\partial(\rho_\ell + \rho_v)}{\partial B} \left[ \frac{\partial(\rho_\ell + \rho_v)}{\partial A} \text{Cov}(A,B) + \frac{\partial(\rho_\ell + \rho_v)}{\partial B} \text{Var}(B) + \frac{\partial(\rho_\ell + \rho_v)}{\partial C} \text{Cov}(B,C) \right] \\
& + \frac{\partial(\rho_\ell + \rho_v)}{\partial C} \left[ \frac{\partial(\rho_\ell + \rho_v)}{\partial A} \text{Cov}(A,C) + \frac{\partial(\rho_\ell + \rho_v)}{\partial B} \text{Cov}(B,C) + \frac{\partial(\rho_\ell + \rho_v)}{\partial C} \text{Var}(C) \right]
\end{aligned} \tag{129}$$

where from eq. (121):

$$\frac{\partial(\rho_\ell + \rho_v)}{\partial A} = 1 ,$$

$$\frac{\partial(\rho_\ell + \rho_v)}{\partial B} = \epsilon^P (\rho_\ell - \rho_v) ,$$

$$\frac{\partial(\rho_\ell + \rho_v)}{\partial C} = \epsilon^R (\rho_\ell - \rho_v) ,$$

obtaining  $\rho_\ell$  and  $\rho_v$  from eqs. (125) and (126) respectively. The variances and covariances are those previously given. The standard deviation of  $(\rho_\ell + \rho_v)$  at each temperature is multiplied by three and the result is plotted to show the  $3\sigma$  confidence limit band. The results are shown in fig. 13.

The behavior of the band deviates from the so-called classical form in the temperature range from about 238 - 250 K. The classical form is found from the latter temperature to the critical. The graph indicates that  $\rho_c$  is found to four significant figures at a high degree of confidence, i.e.,

$$7.62921 \leq \rho_c \leq 7.62937 \text{ (mol/dm}^3\text{)}$$

within a  $3\sigma$  confidence band.

Finally an analysis of the effect of the data weights on the  $\rho_c$  value was made. The unweighted fit of  $X_{LV,c}$  resulted in a value of  $\rho_c = 7.629 \text{ (mol/dm}^3\text{)}$  to four significant figures with a slightly higher variance of the data. All in all, the value of  $\rho_c$ , found by the fit of  $X_{LV,c}$  to the saturation data, results in a statistically reliable number. The foregoing analysis supports the use of the  $X_{LV,c}$  method to obtain a correlated  $\rho_c$  from saturation data.

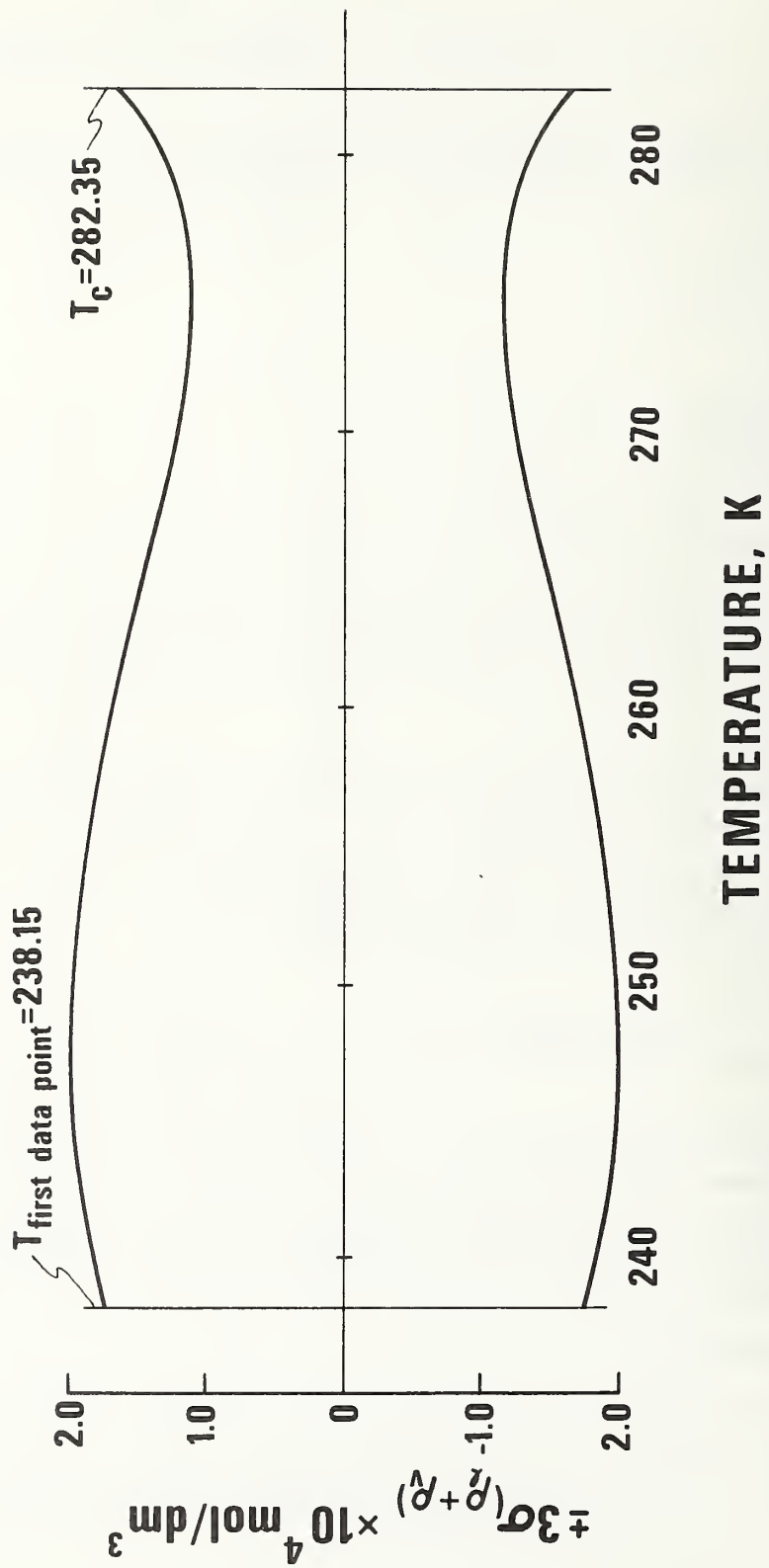


Figure 13.  $3\sigma$  Confidence Limit Band on  $\rho_{\ell} + \rho_v$  of Ethylene.

## 5. EXPERIMENTAL APPROACH TO SIMULTANEOUS DETERMINATION OF COEXISTENCE DATA

This section presents a method for obtaining saturation density data simultaneously. Current experimental approaches obtain  $\rho_\ell$  and  $\rho_v$  in separate experiments. Usually the  $\rho_\ell$  is obtained directly while the  $\rho_v$  is found from the intersection of isochores with the vapor pressure curve. See Kleinrahm, et al. [15] for a review of these techniques.

The method proposed here is based on the straight line plots found in fig. 5. Theoretically, all one needs to know is two pairs of liquid volume fraction - total density data at the same temperature to establish a line. Simple extrapolation to  $X_{LV} = 1$  for  $\rho_\ell$  and to  $X_{LV} = 0$  for  $\rho_v$  produces the saturation values from the same set of data. This should enhance internal consistency.

Currently, in many cases, the coexistence data takes a secondary role in property fitting to equations of state. For example, the procedure used by Haar, et al. [9] for ammonia is to obtain the saturation data from a surface described by an equation of state explicit in Helmholtz free energy. The coexistence data (mainly those of Cragoe, et al. [10,11] were used only to obtain estimates of the critical properties. Perhaps a more internally consistent set of  $\rho_v$ ,  $\rho_\ell$  data can provide the foundation for an equation of state.

To test the validity of using data such as that illustrated in fig. 5, liquid volume fraction data is needed. Unfortunately, the thermodynamic property literature yields very little total density-liquid volume fraction information. However, Cragoe, et al. [10,11] in obtaining  $\rho_\ell$  and  $\rho_v$  for ammonia did measure and publish such data. They did not use them, however, in the manner suggested here. To test this idea, one needs saturated liquid and vapor density values data at the same temperature. Unfortunately, this occurs at only one point in all the data taken by Cragoe and his co-workers. In their report on the liquid densities [10] at  $T = -46.43^\circ\text{C}$  the values are:

$$\rho_T = .5370715 \text{ g/cm}^3, \text{ and}$$

$$X_{LV} = .7695038$$

and in the vapor density report [11] at  $T = -46.42^\circ\text{C}$  the values of

$$\rho_T = .0037965898 \text{ g/cm}^3, \text{ and}$$

$$X_{LV} = .0047679271,$$

are given. These two points determine a straight line. Then  $X_{LV} = 0$  is substituted to obtain  $\rho_v$ , and  $X_{LV} = 1$  is substituted to obtain  $\rho_\ell$ . See fig. 14 for a sketch of the data and procedure. (Because of the relative sizes of the numbers, they are not plotted precisely on the linear scales.)

Table 12 gives some comparisons related to the data in fig. 14. The first column gives the results from the straight line. The second column gives the experimental values of Cragoe, et al. [10,11] while the third column gives the values of Haar, et al. [9] linearly interpolated to  $-46.425^\circ\text{C}$ .

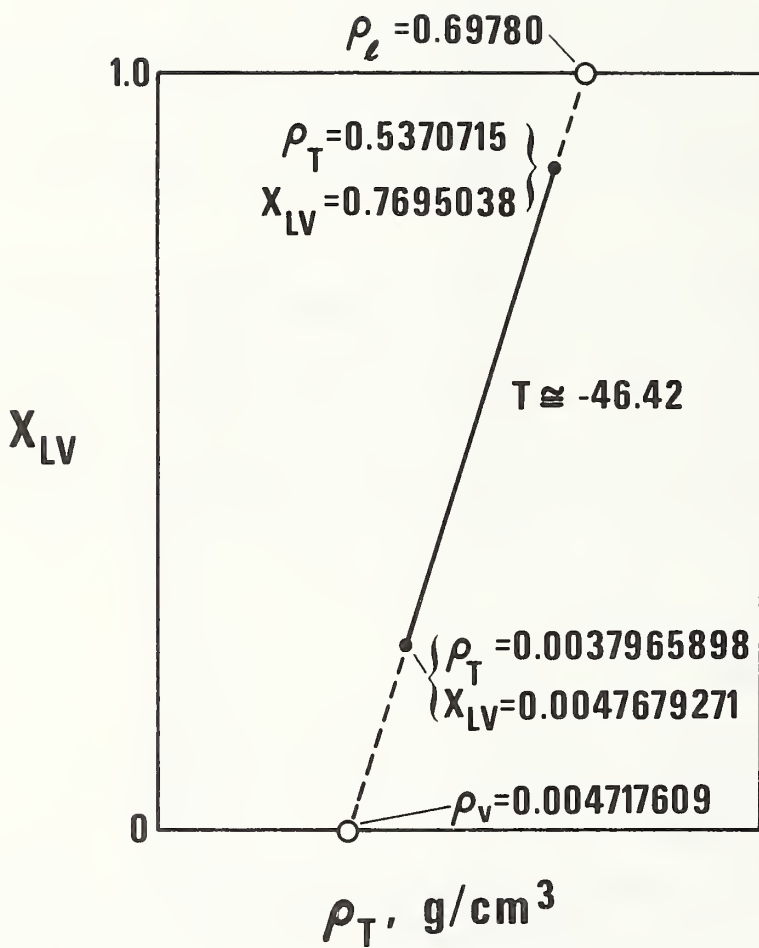


Figure 14.  $X_{LV}$  vs  $\rho_T$  to Find  $\rho_L$  and  $\rho_V$  for Ammonia.

Table 12. Comparison of Coexistence Densities (g/cm<sup>3</sup>)

This Report - Straight Line Method	Cragoe, et al. [10,11] Experimental	Haar, et al. [9]. Equation of State
$\rho_v = .0004717609$	$\rho_v = .0004726344$ (T = -46.42°C)	$\rho_v = .000462$ (T = -46.425°C)
$\rho_\ell = .69780$	$\rho_\ell = .69781$ (T = -46.43°C)	$\rho_\ell = .69770$ (T = -46.425°C)

Another approach which could be taken would be to utilize accurate  $\rho_\ell$  data ( $X_{LV} = 1$ ) along with ( $X_{LV} < 1, \rho_T$ ) data and obtain a straight line. This line could be extrapolated to  $X_{LV} = 0$  to obtain a value for  $\rho_v$ . This was done utilizing data presented by Cragoe, et al. [10] in their report on liquid densities only.

The results are presented in table 13. Data is taken from Haar, et al. [9] at the nearest even temperature for comparison. A  $\rho_{v,CALC}$  is found at the same temperature from the equations presented in Cragoe, et al. [11] when dealing only with  $\rho_v$ . The values for  $\rho_v$  in table 13 not only reflect the range of error involved in  $\rho_v$  determination but also the wide disagreement as to what the  $\rho_v$  actually are. The straight line values for  $\rho_v$  are at least correlated with the experimental  $\rho_\ell$  values.

If the  $\rho_v$  is specified along with a point ( $X_{LV} < 1, \rho_T$ ),  $\rho_\ell$  can be determined from the straight line at  $X_{LV} = 1$ . Here the results are even more surprising. For very small  $X_{LV}$  ( $\sim .005$ ) there is good agreement in the  $\rho_\ell$  values at  $X_{LV} = 1$ . See table 14.

Table 13. Comparison of  $\rho_v$  Values ( $\text{g}/\text{cm}^3$ )

T ( $^{\circ}\text{C}$ )	$\rho_{\ell,\text{DATA}}$	$\rho_{\text{T},\text{DATA}}$	$X_{\text{LV},\text{DATA}}$	$\rho_{v,\text{STR}} \times 10^4$ Line	$\rho_{v,\text{CALC}} \times 10^4$	$\rho_{v,\text{PUB}} \times 10^4$
Cragoe (Haar)	Cragoe [10]				Cragoe [11]	Haar [9]
-49.96 (-50)	.702099	.576546	.821076	3.8557	3.8243	3.8100
-40.14 (-40)	.690255	.57690	.835630	6.2074	6.4057	6.440
-30.04 (-30)	.677782	.540417	.797018	10.454	10.367	10.380
-14.94 (-15)	.658592	.57627	.87464	18.977	19.706	19.670
-00.05 (0)	.638590	.553245	.865617	35.023	34.467	34.580
+10.00 (10)	.624637	.553035	.884468	48.793	48.594	48.680
+20.01 (20)	.610273	.55291	.904958	67.099	66.896	67.010
+29.98 (30)	.595295	.55275	.927413	91.772	90.258	90.050
+39.94 (40)	.579606	.53600	.923170	119.52	119.86	120.29
+49.94 (50)	.562905	.495826	.877389	158.24	157.36	157.80
+60.22 (60)	.544802	.536281	.98373	208.72	206.08	204.90
+80.58 (81)	.504322	.449203	.882783	340.94	345.88	347.44
+91.24 (91)	.479773	.44896	.929207	444.78	453.74	445.80

Table 14. Comparison of  $\rho_{\ell}$  Values ( $\text{g}/\text{cm}^3$ )

T ( $^{\circ}\text{C}$ )	$\rho_{v,\text{DATA}} \times 10^3$	$\rho_{\text{T},\text{DATA}} \times 10^3$	$X_{\text{LV},\text{DATA}}$	$\rho_{\ell,\text{STR}}$ Line	$\rho_{\ell,\text{CALC}}$	$\rho_{\ell,\text{PUB}}$
Cragoe (Haar)	Cragoe [11]				Cragoe [10]	Haar [9]
-50.00 (-50)	.390442	3.6784	.004687	.701877	.701997	.70202
-42.07 (-42)	.585035	3.8702	.004748	.692422	.692486	.69231
-32.99 (-33)	.905551	3.8694	.004356	.681302	.681370	.68122
-17.88 (-18)	1.76246	7.5843	.008815	.662238	.662279	.66232
-03.09 (-3)	3.10183	6.9142	.005960	.642766	.642762	.64267
+02.98 (+3)	3.84438	3.9526	.000172	.634123	.634480	.63454
+24.05 (24)	7.57576	14.6599	.011873	.604227	.604249	.60448
+32.03 (32)	9.58130	16.3919	.011693	.592041	.592090	.59227
+46.32 (46)	14.2653	14.6496	.000693	.568489	.569091	.56967

The results shown in tables 12, 13, 14, may motivate experimentalists to obtain coexistence data from  $(\rho_{\text{T}}, X_{\text{LV}})$  plots. Cragoe, although he did not use the above method, did measure liquid volume fractions using sight lines determined by careful volumetric calibration. (In evaluating the coexistence data of ammonia, Haar, et al. [9] concludes that the data of Cragoe, et al. [10,11] is the best-indicating that accurate measurements can be made of the liquid volume fraction.)

An even earlier effort than Cragoe's to determine saturation densities by measuring liquid volumes is that of Young [16]. He utilized pairs of measured liquid volumes and total mass values in calculations based on mass balances. The approach is similar in concept to the ideas expressed in figs. 5 and 14 of this paper. He did not utilize, however, the reduced variable form, i.e., liquid volume fraction vs. total density nor did he explore the implication of these as thermodynamic functions as is done in this report.

An examination of fig. 5, indicates that these lines should be significantly different (statistically speaking) over a small range of temperature just below the critical. This is in contrast to the (P vs T) isochores near the critical point which are extrapolated to the vapor pressure to find  $\rho_v$ . When utilizing the  $X_{LV}$  vs  $\rho_T$  plots to obtain coexistence data it appears that the large changes in  $\rho_\ell$  and  $\rho_v$  near the critical point may actually be helpful, whereas up to this time these changes were a problem.

The goal then is to obtain a good measurement of the liquid level. Aside from the visual method utilized by Cragoe, newer techniques such as time-domain reflectometry [17] or fiber optics [18] should be investigated.

## 6. SUMMARY

An analysis of the liquid volume and liquid mass fractions has been made over the temperature range from the triple point to the critical point. Limits of the functions and derivatives have been studied both at the triple and critical points. Also the slope of the rectilinear diameter at the critical was studied in some detail. Conclusions were made about the constants and exponents in the  $\rho_\ell$  and  $\rho_v$  coexistence dome equations. A procedure for correlating saturation data with the critical point has been presented using ethylene as an example. Finally, an experimental approach for obtaining  $\rho_\ell$  and  $\rho_v$  simultaneously is presented.

## 7. ACKNOWLEDGMENTS

I wish to thank the staff of the Thermophysical Properties Division of the National Bureau of Standards, Boulder, Colorado for making office, digital computer, and data resources available during my tenure as a guest worker. Thanks also to those staff members who took the time for stimulating discussions, especially Robert McCarty regarding the statistical analysis of the  $X_{LV,c}$  fit. Salary support was provided by Calvin College, Grand Rapids, Michigan during my Sabbatical leave.

## 8. REFERENCES

- [1] Methane, International Thermodynamic Tables of the Fluid State-5, 1976, IUPAC, Chemical Data Series, No. 16, Pergamon Press, Oxford.
- [2] Hohenberg, P. C. and Barmatz, M., 1972, Gravity Effects Near the Gas-Liquid Critical Point, *Phys. Rev. A*, 6: 289-313.
- [3] Green, M. S., Cooper, M. J. and Sengers, J. M. H. Levelt, 1971, Extended Thermodynamic Scaling From a Generalized Parametric Form, *Phys. Rev. Lett.*, 26: 492-495.
- [4] Sengers, J. M. H. Levelt, Straub, J. and Vincenti-Missoni, M. J., 1971, Coexistence Curves of CO<sub>2</sub>, N<sub>2</sub>O and CClF<sub>3</sub> in the Critical Region, *J. Chem. Phys.* 54: 5034-5050.
- [5] Moldover, M. R., 1974, Visual Observation of the Critical Temperature and Density: CO<sub>2</sub> and C<sub>2</sub>H<sub>4</sub>, *J. Chem. Phys.*, 61: No. 5, 1766-1778.
- [6] Van Poolen, Lambert John, 1977, Analysis of Property Data in the Critical Region Using the Function-Liquid Volume Fraction, *ASHRAE Transactions*, 8: Part II, Dec.
- [7] Weber, Lloyd A., 1970, Density and Compressibility of Oxygen in the Critical Region, *Phys. Rev. A*, 2: No. 6, 2379-2388.
- [8] Douslin, D. R. and Harrison, R. H., 1976, Pressure, Volume, Temperature Relations of Ethylene, *J. Chem. Thermodynamics*, 8: 301-330.
- [9] Haar, L. and Gallagher, J. S., 1978, Thermodynamic Properties of Ammonia, *J. Phys. Chem. Ref. Data*, 7: No. 3, 635-792.
- [10] Cragoe, C. S. and Harper, 3rd, D. R., 1921, Specific Volume of Liquid Ammonia, *Scientific Papers of the Bureau of Standards*, Vol 17, 287-315.
- [11] Cragoe, C. S., McKelvey, E. C. and O'Connor, G. F., 1922, Specific Volume of Saturated Ammonia Vapor, *Scientific Papers of the Bureau of Standards*, Vol 18, 707-735 (dated 3/17/23).
- [12] Weiner, J., Langley, K. H. and Ford, N. C., Jr., 1974, Experimental Evidence for a Departure from the Law of the Rectilinear Diameter, *Phys. Rev. Lett.*, 32: No. 16, 879-886.
- [13] Gosman, A. L., McCarty, R. D. and Hust, J. G., 1969, Thermodynamic Properties of Argon From the Triple Point to 300 K at Pressures to 1000 Atmospheres, *NSRDS-NBS Report No. 27*.
- [14] Sengers, J. M. H. Levelt, private communication, 1979.
- [15] Kleinrahm, R. and Wagner, W., 1978, Examination of Density Measuring Procedures and Design of Device for Precise Measurement of Boiling and Thawing Densities, *Chem. Ing. Tech.*, 50: No. 10, 805 (synopsis)(in German).
- [16] Young, S., 1910, The Vapor-Pressures, Specific Volumes, Heats of Vaporization, and Critical Constants of Thirty Pure Substances, *Scientific Proceedings, Royal Dublin Society*, 12: 374-443, June 10.

- [17] Cruz, J. E., Rogers, E. H. and Heister, A. E., 1973, Continuous Liquid Level Measurements with Time-Domain Reflectometry, Paper H-4, Advances in Cryogenic Engineering, Vol 18, Plenum Press, N. Y., 323-327.
- [18] Elson, B. M., 1978, Fiber Optics Technology Investigated, Aviation Week and Space Tech (Oct. 16).

## APPENDIX A. Symbols and Units

A	constant
B	constant
b	constant
C	constant
c	constant
Cov	covariance
m	mass
P	pressure, EXPONENT
R	exponent
T	temperature
V	volume
Var	variance
X	$0 \leq \text{fraction} \leq 1$
X'	mass or volume fraction derivative with respect to temperature
$\beta$	exponent
$\epsilon$	$T_c - T$
$\phi$	exponent
$\psi$	exponent
$\rho$	density
$\rho'$	density derivative with respect to temperature
$\sigma$	standard deviation

### SUBSCRIPTS

c	critical point
c,LIM	critical point, limit
l	saturated liquid
LM	liquid mass
LV	liquid volume
MAX	point at which $X_{LV}$ has a maximum
MIN	point at which $X_{LM}$ has a minimum
SAT	saturation
T	total or overall
TP	triple point
v	saturated vapor
1	related to constant modifying $\epsilon^\beta$ term
2	related to constant modifying $\epsilon^\phi$ term
3	related to constant modifying $\epsilon^\psi$ term

### SUPERSCRIPTS

-	limit from below
+	limit from above

U.S. DEPT. OF COMM. BIBLIOGRAPHIC DATA SHEET	1. PUBLICATION OR REPORT NO.  NBSIR 80-1631	2. Gov't. Accession No.	3. Recipient's Accession No.
4. TITLE AND SUBTITLE  ANALYSIS OF LIQUID VOLUME AND LIQUID MASS FRACTIONS AT COEXISTENCE FOR PURE FLUIDS		5. Publication Date  May 1980	
7. AUTHOR(S)  Lambert John Van Poolen		8. Performing Organization Report No.	
9. PERFORMING ORGANIZATION NAME AND ADDRESS  NATIONAL BUREAU OF STANDARDS DEPARTMENT OF COMMERCE WASHINGTON, DC 20234		10. Project/Task/Work Unit No.  [REDACTED]	
12. SPONSORING ORGANIZATION NAME AND COMPLETE ADDRESS (Street, City, State, ZIP)		13. Type of Report & Period Covered  [REDACTED]	
15. SUPPLEMENTARY NOTES  <input type="checkbox"/> Document describes a computer program; SF-185, FIPS Software Summary, is attached.			
16. ABSTRACT (A 200-word or less factual summary of most significant information. If document includes a significant bibliography or literature survey, mention it here.)  An analysis of the behavior of liquid volume and liquid mass fractions at coexistence for pure fluids is made. Scaled equations for the saturation liquid and vapor densities are analyzed and relationships between various exponents and among constant coefficients are presented. Inequalities which exist among the saturation densities and their derivatives are developed. A procedure to correlate saturation data with the critical point is applied to ethylene. An experimental procedure to determine, simultaneously, saturated liquid and vapor densities at a given temperature is presented.			
17. KEY WORDS (six to twelve entries; alphabetical order; capitalize only the first letter of the first key word unless a proper name; separated by semicolons)  Coexistence densities; critical density; critical point; liquid mass fraction; liquid volume fraction; phase equilibria; pure fluids.			
18. AVAILABILITY  <input checked="" type="checkbox"/> Unlimited  <input type="checkbox"/> For Official Distribution. Do Not Release to NTIS  <input type="checkbox"/> Order From Sup. of Doc., U.S. Government Printing Office, Washington, DC 20402, SD Stock No. SN003-003-  <input checked="" type="checkbox"/> Order From National Technical Information Service (NTIS), Springfield, VA, 22161		19. SECURITY CLASS (THIS REPORT)  UNCLASSIFIED	21. NO. OF PRINTED PAGES  63
		20. SECURITY CLASS (THIS PAGE)  UNCLASSIFIED	22. Price  \$7.00





